The Plant Cell, Vol. 31: 663–686, March 2019, www.plantcell.org © 2018 ASPB.

The AREB1 Transcription Factor Influences Histone Acetylation to Regulate Drought Responses and Tolerance in *Populus trichocarpa*[OPEN]

Shuang Li,[a,1] Ying-Chung Jimmy Lin,[a,b,c,1] Pengyu Wang,[a] Baofeng Zhang,[a] Meng Li,[a] Su Chen,[a] Rui Shi,[b,d] Sermsawat Tunlaya-Anukit,[b] Xinying Liu,[a] Zhifeng Wang,[a] Xiufang Dai,[a] Jing Yu,[a] Chenguang Zhou,[a] Baoguang Liu,[a] Jack P. Wang,[a,b] Vincent L. Chiang,[a,b,2] and Wei Li[a,2]

[a] State Key Laboratory of Tree Genetics and Breeding, Northeast Forestry University, Harbin 150040, China
[b] Forest Biotechnology Group, Department of Forestry and Environmental Resources, North Carolina State University, Raleigh, North Carolina 27695
[c] Department of Life Sciences and Institute of Plant Biology, College of Life Science, National Taiwan University, Taipei 10617, Taiwan
[d] Department of Crop and Soil Science, North Carolina State University, Raleigh, North Carolina 27695

ORCID IDs: 0000-0003-2352-2904 (S.L.); 0000-0001-7120-4690 (Y.-C.J.L.); 0000-0002-0595-7018 (P.W.); 0000-0002-1675-6940 (B.Z.); 0000-0002-3611-3731 (M.L.); 0000-0002-8814-5444 (S.C.); 0000-0001-9070-1369 (R.S.); 0000-0001-6046-3136 (S.T.-A.); 0000-0002-9737-0897 (X.L.); 0000-0002-1153-4337 (Z.W.); 0000-0002-8419-4230 (X.D.); 0000-0001-5761-4079 (J.Y.); 0000-0001-6414-4693 (C.Z.); 0000-0002-0282-0083 (B.L.); 0000-0002-5392-0076 (J.P.W.); 0000-0002-7152-9601 (V.L.C.); 0000-0002-4407-9334 (W.L)

Plants develop tolerance to drought by activating genes with altered levels of epigenetic modifications. Specific transcription factors are involved in this activation, but the molecular connections within the regulatory system are unclear. Here, we analyzed genome-wide acetylated lysine residue 9 of histone H3 (H3K9ac) enrichment and examined its association with transcriptomes in *Populus trichocarpa* under drought stress. We revealed that abscisic acid-Responsive Element (ABRE) motifs in promoters of the drought-responsive genes *PtrNAC006*, *PtrNAC007*, and *PtrNAC120* are involved in H3K9ac enhancement and activation of these genes. Overexpressing these *PtrNAC* genes in *P. trichocarpa* resulted in strong drought-tolerance phenotypes. We showed that the ABRE binding protein PtrAREB1-2 binds to ABRE motifs associated with these *PtrNAC* genes and recruits the histone acetyltransferase unit ADA2b-GCN5, forming AREB1-ADA2b-GCN5 ternary protein complexes. Moreover, this recruitment enables GCN5-mediated histone acetylation to enhance H3K9ac and enrich RNA polymerase II specifically at these *PtrNAC* genes for the development of drought tolerance. CRISPR editing or RNA interference-mediated downregulation of any of the ternary members results in highly drought-sensitive *P. trichocarpa*. Thus, the combinatorial function of the ternary proteins establishes a coordinated histone acetylation and transcription factor-mediated gene activation for drought response and tolerance in *Populus* species.

INTRODUCTION

Drought severely affects plant growth, forest productivity, and survival throughout the world. Under drought stress, stem hydraulic conductance and aboveground biomass production decrease, causing an up to 45% reduction in radial growth in many forest species (Barber et al., 2000). Severe water deprivation leads to death (Choat et al., 2012). *Populus* species, widely distributed across the northern hemisphere, are among the most drought-sensitive woody species (Monclus et al., 2006), but their wood is a preferred renewable resource for biomaterials and bioenergy production (Ragauskas et al., 2006). Drought-tolerant genotypes of these species could influence the bioeconomy worldwide. Understanding the genetic and regulatory mechanisms of drought response and tolerance in *Populus* will enable effective strategic engineering of novel robust genotypes.

Plants respond and adapt to drought stress by transcriptionally reprogramming networks of gene expression regulated by a subset of differentially activated or repressed transcription factors (TF; Nakashima et al., 2014; Song et al., 2016). The differential expression of such TFs is typically the result of changes in the levels of specific epigenetic modifications on the genes for these TFs through stress signal transduction (Jaenisch and Bird, 2003; Kouzarides, 2007). Epigenetic marks are covalent modifications of chromatin, such as histone acetylation and methylation, that initiate and maintain the activities of TFs (Norton et al., 1989; Lee et al., 1993; Shahbazian and Grunstein, 2007; Zentner and Henikoff, 2013).

Acetylated Lys residue 9 of histone H3 (H3K9ac) is one of the most extensively studied epigenetic marks in vascular plants (Kim et al., 2008; Charron et al., 2009; Zhou et al., 2010; Li et al., 2011). Hyperacetylation of H3K9 is almost invariably associated with the activation of transcription in all species studied so far, whereas hypoacetylated histones are accompanied by transcriptional repression (Shahbazian and Grunstein, 2007; Zhou et al., 2010; Li et al., 2011; Zentner and Henikoff, 2013). H3K9ac has been considered a general chromatin marker of gene activation.

[1] These authors contributed equally to this work.
[2] Address correspondence to vchiang@ncsu.edu or weili2015@nefu.edu.cn.
The authors responsible for distribution of materials integral to the findings presented in this article in accordance with the policy described in the Instructions for Authors (www.plantcell.org) are: Vincent L. Chiang (vchiang@ncsu.edu) and Wei Li (weili2015@nefu.edu.cn).
[OPEN] Articles can be viewed without a subscription.
www.plantcell.org/cgi/doi/10.1105/tpc.18.00437

IN A NUTSHELL

Background: Plants may become drought tolerant by activating specific drought-responsive genes. Many such genes are chemically modified with so-called epigenetic marks, such as H3K9ac (acetylation of a specific histone). Two key steps coordinate the activation of the drought-responsive genes. One is an increase in the H3K9ac marks. The other involves a protein transcription factor (TF) binding to the drought-responsive gene for activation. We know that ABSCISIC ACID-RESPONSIVE ELEMENT BINDING (AREB) protein, a TF, has such a unique capability. We also know that the H3K9ac marks can be increased by a catalytic system containing a histone acetyltransferase (HAT) enzyme. However, we don't know how these two steps are coordinated for gene activation.

Question: We wanted to know how H3K9ac modification is linked to AREB TF function for the activation of drought-responsive genes. More specifically, we wanted to know what system catalyzes the increase of the H3K9ac mark and how this system is brought specifically to the drought-responsive genes through AREB TF activation.

Findings: We identified three drought-responsive genes (*PtrNAC006*, *PtrNAC007*, and *PtrNAC120*) in *Populus trichocarpa* under drought stress. They had increased H3K9ac marks and contained the sequences for AREB TF binding. We further identified PtrAREB1 as a TF that could bind to these *PtrNAC* genes. We found that while bound to the *PtrNAC* gene, PtrAREB1 recruited a HAT (termed GCN5) containing a protein dimer, ADA2b-GCN5, forming a trimer, PtrAREB1-ADA2b-GCN5. Binding of this trimer to the *PtrNAC* gene increased its H3K9ac and expression levels. High level expression of these *PtrNAC* genes in *P. trichocarpa* resulted in strong drought-tolerance phenotypes. Therefore, we revealed a catalytic system for the H3K9ac mark and how this system is specifically brought to the AREB TF for gene activation to develop drought tolerance in *Populus*.

Next steps: This study uncovered a coordinated regulation of H3K9ac and AREB TF functions for developing drought tolerance in *Populus*. Knowledge of how this regulation interacts with other regulatory systems will be important for future breeding of trees with maximized growth and other properties to support a sustainable ecosystem.

Consistent with this, the euchromatin (where DNA is accessible for transcription) of many eukaryotes, including plants, is marked by H3K9ac (Kurdistani et al., 2004; Kouzarides, 2007; Shahbazian and Grunstein, 2007). H3K9ac is enriched in response to drought stress in Arabidopsis (*Arabidopsis thaliana*), and this enrichment correlates with transcriptional activation for four drought-responsive genes, *RD29A*, *RD29B*, *RD20*, and *At2g20880* (Kim et al., 2008, 2012). Importantly, rehydration rapidly removes drought-induced H3K9ac enrichment from regions of these genes (Kim et al., 2012). Chromatin immunoprecipitation sequencing (ChIP-seq) analysis of chromatin modifications in the genome of the moss *Physcomitrella patens* similarly demonstrated that H3K9ac patterns respond dynamically to dehydration stress (Widiez et al., 2014).

Histone acetylation is catalyzed by histone acetyltransferase (HAT) complexes (Shahbazian and Grunstein, 2007), many of which contain GENERAL CONTROL NON-DEREPRESSIBLE5 (GCN5) as the catalytic subunit (Brownell et al., 1996) and ALT ERATION/DEFICIENCY IN ACTIVATION2 (ADA2) as an adaptor protein (Grant et al., 1997). ADA2 increases the HAT activity of GCN5 (Balasubramanian et al., 2002). Arabidopsis contains two related ADA2 factors, ADA2a and ADA2b (Stockinger et al., 2001). *ada2b* mutants are hypersensitive to salt stress and abscisic acid (ABA; Hark et al., 2009), suggesting that ADA2b is involved in the abiotic stress response. Mutations in GCN5 and ADA2 affect the expression of several cold-regulated genes leading to reduced tolerance to freezing temperatures (Vlachonasios et al., 2003). GCN5 and ADA2 are required for root meristem development in Arabidopsis and rice (*Oryza sativa*; Kornet and Scheres, 2009; Zhou et al., 2017). GCN5-mediated histone acetylation plays important roles in regulating the transcriptional responses necessary for growth and adaptation to abiotic stress.

Transcriptional responses to drought stress in plants involve TFs, mostly members of the bZIP, NAC, AP2/ERF, MYB, and MYC TF families (Nakashima et al., 2014). ABA-Responsive Element Binding (AREB, also named ABF) proteins of the bZIP family have been characterized extensively for their roles in regulating drought stress responses. The AREB TF binds to the ABA-Responsive Element (ABRE: PyACGTGG/TC) in the promoters of drought-responsive genes, activating the expression of these genes for drought tolerance (Fujita et al., 2011). Transgenic Arabidopsis overexpressing *AREB1/ABF2*, *AREB2/ABF4*, and *ABF3* exhibits enhanced drought tolerance (Fujita et al., 2005, 2011). Arabidopsis plants overexpressing TF and other genes with ABRE motif-containing promoters, such as *ANAC002/ATAF1* (Wu et al., 2009), *ANAC019*, *ANAC055* (Tran et al., 2004; Hickman et al., 2013), *ANAC072/RD26* (Fujita et al., 2004; Tran et al., 2004), *GBF3* (Fujita et al., 2005; Ramegowda et al., 2017), *HIS1-3* (Ascenzi and Gantt, 1999), *RD20* (Aubert et al., 2010), and *RD29B* (Msanne et al., 2011), also show increased drought tolerance. It is well established that drought tolerance is developed through the activation of ABRE-associated genes and that H3K9ac enrichments at such genes are positively correlated with the activation of these genes; however, there has long been a missing link between the two regulatory mechanisms. It remains unclear what system catalyzes the enrichment of H3K9ac modifications and how this system is brought specifically to genes with ABRE-containing promoters. Knowledge of the regulatory mechanisms that initiate and determine drought responses and tolerance is lacking for plants, particularly for tree species.

Wood is made up of xylem, the conductive tissue that transports water from soil to leaves and provides mechanical support for the entire plant (Evert, 2006). Stem xylem vessels are highly vulnerable

to drought-induced cavitation, which causes the interruption of water transport through xylem and stomatal closure leading to a rapid reduction of photosynthesis (Tyree and Sperry, 1989; Arango-Velez et al., 2011). Stem differentiating xylem (SDX) is rich in signaling events and gene transregulation machineries associated with drought response and tolerance (Bogeat-Triboulot et al., 2007; Berta et al., 2010). Therefore, stem xylem is a unique biological system in which to learn about regulatory mechanisms of drought response and tolerance.

In this study, we used *Populus trichocarpa* for soil-water depletion experiments and analyzed SDX tissue by ChIP-seq and RNA sequencing (RNA-seq) for genome-wide H3K9ac distribution and gene expression. We then identified 76 drought-responsive TF genes whose expression was affected by the differential modification of H3K9ac in their promoters, where we found that the ABRE sequence was the most significantly differentially enriched ($P < 10^{-24}$) motif. The 76 ABRE-containing TFs included a subset of *NAC* genes, among which we focused on three (*PtrNAC006*, *PtrNAC007*, and *PtrNAC120*) and demonstrated that they induce strong drought-tolerant phenotypes when overexpressed in transgenic *P. trichocarpa*. We identified a coordinated regulation of histone acetylation and TF-mediated gene activation in drought response and tolerance. Binding of trimeric AREB1-ADA2b-GCN5 protein complexes to ABRE motifs in promoters of drought-responsive genes, such as the three *PtrNAC* genes, elevated their H3K9ac levels and RNA polymerase II (Pol II) recruitment, leading to activation of the *PtrNAC* genes and increasing drought tolerance. This coordinated regulation required the combinatorial function of AREB1, ADA2b, and GCN5 proteins.

RESULTS

The H3K9ac Profile Changes in SDX Tissue of *P. trichocarpa* in Response to Drought

To gain insight into the role of H3K9ac modifications in drought response, we generated genome-wide H3K9ac profiles for 3-month-old control and drought-treated *P. trichocarpa* plants maintained in a greenhouse (Supplemental Figure 1). Pilot drought experiments suggested that 5-d (D5) and 7-d (D7) drought treatments together would most likely induce changes in the greatest number of genes most highly responsive to drought stress (Supplemental Figures 1A and 1B). Therefore, we applied these two treatments for subsequent ChIP-seq and RNA-seq analyses. We performed ChIP-seq on SDX tissue collected from plants with regular watering (control, no drought [ND]) (Supplemental Figures 1C and 1D) and plants under drought treatment (soil-water depletion) for 5 and 7 d (Supplemental Figures 1C and 1D; see Methods). The SDX tissue collection from the control (ND) and the drought-treated (D5 and D7) plants was conducted on the same day and at the same time (Supplemental Figure 1C). ChIP-seq was conducted using antibodies against H3K9ac according to the protocol developed for woody species (Lin et al., 2013; Li et al., 2014). We used diffReps (Shen et al., 2013) to identify differential H3K9ac-modified genomic regions (peaks) between 5-d drought and control plants (D5/ND) and between 7-d drought and control plants (D7/ND). We found 4578 peaks with increased and 5081 peaks with decreased H3K9ac modification for D5/ND and 5530 peaks with increased and 5399 peaks with decreased H3K9ac modification regions for D7/ND (adjusted $P < 0.05$, Benjamini-Hochberg adjusted P value in diffReps analysis) (Supplemental Table 1). These results are consistent with the involvement of H3K9ac modifications in drought response in *Physcomitrella patens* (Widiez et al., 2014) and Arabidopsis (Kim et al., 2008, 2012) and provide evidence of such involvement in a tree species.

In each of the 19 *P. trichocarpa* chromosomes, these differential H3K9ac peaks were located mainly in genic regions and were relatively rare in intergenic regions (Supplemental Figures 2A and 2B). The percentage of differential H3K9ac peaks on each chromosome was correlated positively with chromosome size (Supplemental Figure 2C). Fewer differential H3K9ac peaks were identified in chromosomal regions where transposable element (TE) density was high (Supplemental Figure 2C); TEs are particularly common in heterochromatic regions of the genome. Fewer peaks also were distributed in putative centromeric regions of the 19 *P. trichocarpa* chromosomes (Supplemental Figure 2C). Differential H3K9ac peaks were distributed evenly across all chromosomal regions except intergenic, TE, and centromeric regions, indicating that H3K9ac alteration occurs preferentially within gene-rich regions in *P. trichocarpa* under drought stress.

Integrative Analysis of ChIP-seq and RNA-seq Data Identifies a Set of Drought Stress-Responsive Genes with Differential H3K9ac

Next, we determined whether the differential H3K9ac enrichments were responsible for regulating gene expression changes in response to drought stress. We performed RNA-seq to characterize transcriptome changes in SDX tissues in response to drought stress (Supplemental Figure 1; see Methods). RNAs used to construct the RNA-seq libraries were extracted from the same SDX tissues used for ChIP-seq analyses. Using edgeR (Robinson et al., 2010) and our analysis pipeline (Lin et al., 2013), we characterized the RNA-seq results to identify differentially expressed genes (DEGs) induced by drought treatments. We found 8341 upregulated and 7118 downregulated genes after 5 d of drought stress (D5/ND; false discovery rate [FDR] < 0.05) and 6334 upregulated and 5394 downregulated genes after 7 d of drought treatment (D7/ND; FDR < 0.05) (Supplemental Figure 3 and Supplemental Table 2). Gene Ontology (GO) analysis (Supplemental Figure 4) showed that the number of genes in nearly all GO categories at D7 was lower than that at D5. In addition, two classes of genes, "regulation of developmental process" and "regulation of growth" (Supplemental Figure 4), were completely absent from D7 data. The absence of these two classes of genes may be a major reason for the difference in DEG numbers between the D5 and D7 treatments.

Using BETA (Wang et al., 2013), we integrated the H3K9ac ChIP-seq data with the RNA-seq data (D5/ND and D7/ND) to identify DEGs exhibiting differential H3K9ac levels (Supplemental Figure 5). We focused on DEGs with differential H3K9ac enrichment in promoter regions (within ± 2 kb of the transcription start site [TSS]; see Methods) to identify genes most likely to be regulated directly by H3K9ac modification (Figures 1A and 1B). There are four possible combinations for the correlation of differential H3K9ac modification and differential gene expression (Figures 1A

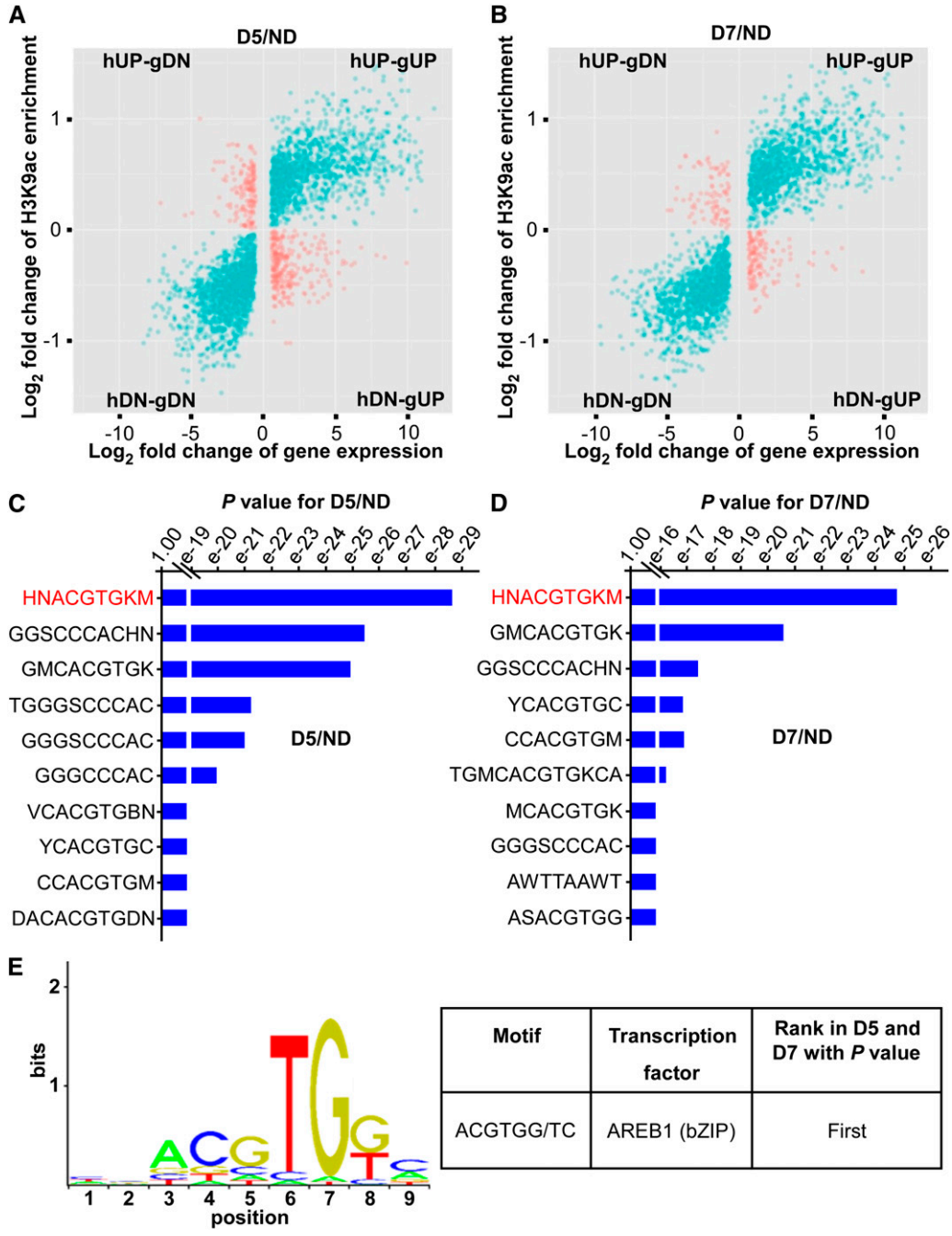

Motif	Transcription factor	Rank in D5 and D7 with *P* value
ACGTGG/TC	AREB1 (bZIP)	First

Figure 1. Integration of ChIP-seq and RNA-seq Data to Identify Drought Stress-Responsive Genes with Differential H3K9ac of Promoters and Identification of Transcription Binding Motifs.

(A) and **(B)** Plots for $\log_2$ fold change of gene expression and H3K9ac enrichment at promoters for D5/ND **(A)** and D7/ND **(B)**.
(C) and **(D)** Analysis of motif enrichment of the promoters with differential H3K9ac for D5/ND **(C)** and D7/ND **(D)**. H represents A or C or T, N represents any base, K represents G or T, and M represents A or C.
(E) The top-ranked motif in the promoters with differential H3K9ac for both D5/ND and D7/ND was the ABRE consensus motif for the AREB1 TF.

and 1B). These combinations are as follows: (1) increased H3K9ac level induces gene downregulation (histone level up-gene down [hUP-gDN]; red dots in Figures 1A and 1B); (2) increased H3K9ac level induces gene upregulation (hUP-gUP; blue dots); (3) decreased H3K9ac level induces gene upregulation (hDN-gUP; red dots); and (4) decreased H3K9ac level induces gene down-regulation (hDN-gDN; blue dots). Because H3K9ac is an activating mark (Kurdistani et al., 2004; Shahbazian and Grunstein, 2007;

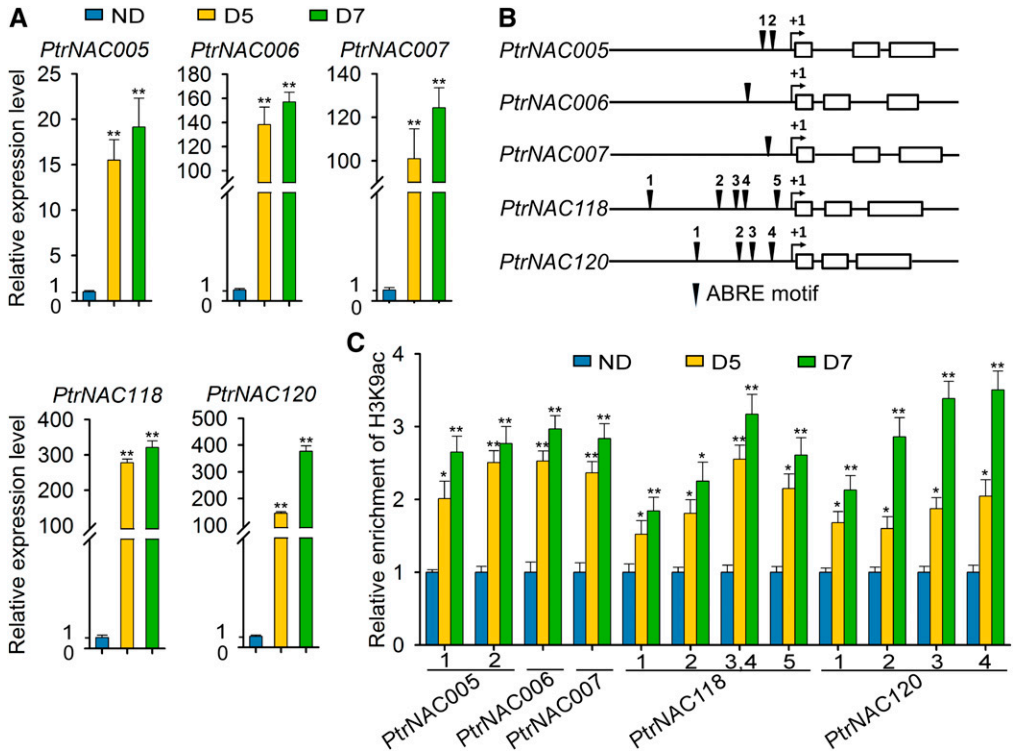

Figure 2. ABRE Motifs Mediate H3K9ac Association and the Regulation of *PtrNAC* Genes.

(A) RT-qPCR detection of *PtrNAC005*, *PtrNAC006*, *PtrNAC007*, *PtrNAC118*, and *PtrNAC120* in wild-type *P. trichocarpa* plants without (ND) or with drought treatment for 5 d (D5) and 7 d (D7). Error bars indicate 1 SE of three biological replicates from independent pools of *P. trichocarpa* SDX tissues. Asterisks indicate significant differences between control (ND) and drought-treated (D5 and D7) samples for each gene (**, $P < 0.01$, Student's *t* test).

(B) Schematic diagram of ABRE motifs in five *PtrNAC* gene promoters.

(C) ChIP-qPCR detection of H3K9ac in ABRE motif regions of *PtrNAC* promoters in wild-type *P. trichocarpa* plants without (ND) or with drought treatment for 5 d (D5) and 7 d (D7). Numbers indicate ABRE motif sites in each gene. ChIP assays were performed using antibodies against H3K9ac, and the precipitated DNA was quantified by qPCR. Enrichment values represent the relative fold change from ND, and error bars indicate 1 SE of three biological replicates from independent pools of *P. trichocarpa* SDX tissues. Asterisks indicate significant differences between control (ND) and drought-treated (D5 and D7) samples for each fragment containing the ABRE motif (*, $P < 0.05$ and **, $P < 0.01$, Student's *t* test).

Charron et al., 2009; Zhou et al., 2010; Li et al., 2011; Zentner and Henikoff, 2013), combinations showing hUP-gUP and hDN-gDN are most likely to represent direct effects on gene expression. Therefore, we focused on the DEGs with the hUP-gUP and hDN-gDN combinations and identified 3994 DEGs (with 4026 modification sites) that exhibited differential H3K9ac levels in the promoter regions (blue dots in Figure 1A) after 5 d of drought treatment (D5/ND; Supplemental Data Set 1) and 3498 DEGs (with 3527 modification sites) after 7 d of drought treatment (D7/ND; blue dots in Figure 1B; Supplemental Data Set 2).

We further analyzed the hUP-gUP and hDN-gDN set of genes by performing GO enrichment analysis of these genes to explore their functional significance. Biological pathways responsive to stimulus, water deprivation, ABA, and ABA-activated signaling pathway were enriched significantly among this hUP-gUP and hDN-gDN set of genes (Supplemental Data Set 3). Many other biological processes, such as cell wall biogenesis and developmental process, also were highly enriched among this gene set. These results suggest that H3K9ac may regulate drought-responsive genes through ABA-dependent regulation and that H3K9ac modifications may systemically influence the expression of the genes with diverse functions associated with drought response and tolerance. Therefore, this gene expression regulation may involve interplay between H3K9ac and TFs.

The ABRE Was Identified in Promoters of Genes with Differential H3K9ac Modifications

TFs are known to regulate their target genes through binding to specific regulatory DNA sequences (*cis*-elements or TF binding motifs). To investigate whether the interplay between H3K9ac and TFs is involved in the transcriptional regulation of drought-response genes, we examined the enrichment of TF binding motifs within the promoters of the 3994 and 3498 DEGs with differential H3K9ac levels after a 5-d drought (D5/ND) and a 7-d drought (D7/ND), respectively, using AME (Analysis of Motif Enrichment; McLeay and Bailey, 2010) motif searches. This analysis revealed that the ABRE motif for the AREB1-type protein (Fujita et al., 2005, 2011) was most significantly enriched within the H3K9ac-associated promoters for both D5/ND ($P < 10^{-28}$, Fisher's

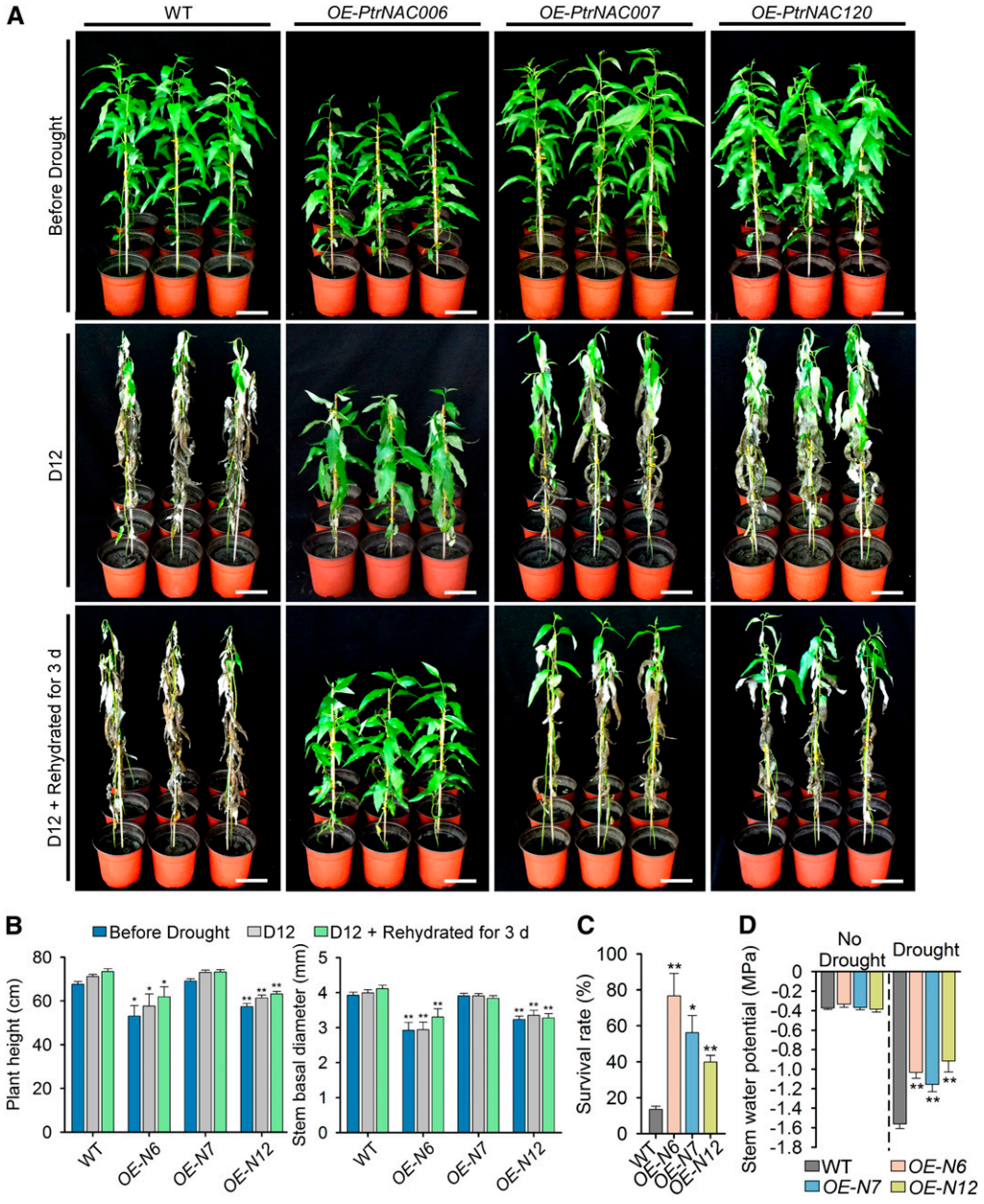

Figure 3. Overexpressing *PtrNAC* Genes Improves the Drought Tolerance of *P. trichocarpa*.

(A) Drought tolerance phenotypes of wild-type and *OE-PtrNAC006*, *OE-PtrNAC007*, and *OE-PtrNAC120* transgenic plants. Three-month-old plants (Before Drought, top row) were dehydrated for 12 d (D12, middle row) and then rehydrated for 3 d (D12 + Rehydrated for 3 d, bottom row). Bars = 10 cm.

(B) Statistical analysis of height and stem basal diameter of wild-type and *OE-PtrNAC006* (*OE-N6*), *OE-PtrNAC007* (*OE-N7*), and *OE-PtrNAC120* (*OE-N12*) transgenic plants before drought, at D12, and at D12 + rehydrated for 3 d. Error bars represent 1 SE of three independent experiments with 12 *P. trichocarpa* plants for each genotype in each replicate. Asterisks indicate significant differences between the transgenics harboring each gene construct and wild-type plants for each time point (*, $P < 0.05$ and **, $P < 0.01$, Student's *t* test).

(C) Statistical analysis of survival rates after drought treatment and recovery (D12 + Rehydrated for 3 d). The average percentage of survival and SE values were calculated from three independent experiments with at least 12 plants of each genotype in each replicate. Asterisks indicate significant differences between the transgenics harboring each gene construct and wild-type plants (*, $P < 0.05$ and **, $P < 0.01$, Student's *t* test).

(D) Statistical analysis of stem water potential of wild-type and *OE-PtrNAC* transgenic plants with no drought treatment and drought treatment for 5 d. Error bars represent 1 SE of three independent experiments with six *P. trichocarpa* plants of each genotype in each replicate, and asterisks indicate significant differences between the transgenics harboring each gene construct and wild-type plants for each condition (**, $P < 0.01$, Student's *t* test).

exact test; sequence in red in Figures 1C and 1E) and D7/ND ($P < 10^{-24}$, Fisher's exact test; sequence in red in Figures 1D and 1E). The ABRE is a *cis*-element that controls the expression of many ABA- and drought-responsive genes in Arabidopsis and many food crops (Nakashima et al., 2014). Our results indicated that ABRE likely plays a similar role in drought response and resistance in a tree species. Therefore, we focused on the ABRE motif to investigate how AREB1 TF binding to ABRE-containing promoters might interplay and coordinate with H3K9ac in response to drought stress. We first identified the relevant genes with ABRE-containing promoters.

ABRE Motifs Mediate H3K9ac Association and Regulation of *PtrNAC* Genes

Activating the expression of ABRE-containing genes encoding TF and non-TF proteins has been shown to induce drought tolerance in Arabidopsis (Ascenzi and Gantt, 1999; Tran et al., 2004; Fujita et al., 2005; Wu et al., 2009; Aubert et al., 2010; Msanne et al., 2011; Hickman et al., 2013; Nakashima et al., 2014; Ramegowda et al., 2017). The induction is particularly effective with the activation of ABRE-containing TFs (Tran et al., 2004; Fujita et al., 2005; Wu et al., 2009; Hickman et al., 2013; Ramegowda et al., 2017). We analyzed our sequence data, focusing on identifying drought-responsive TF DEGs that had the ABRE motif as well as differential H3K9ac levels in their promoters. We found 60 and 53 such TF genes after 5-d (D5/ND; Supplemental Data Set 4) and 7-d (D7/ND; Supplemental Data Set 5) drought treatments, respectively. Among these 113 (60 + 53) TF genes, 37 were common to both the D5 and D7 treatments (highlighted in gray in Supplemental Data Sets 4 and 5), 23 were specific at D5 (highlighted in yellow in Supplemental Data Set 4), and 16 were specific at D7 (highlighted in blue in Supplemental Data Set 5). Thus, there were 76 unique TF genes among these 113 TF genes. While these 76 drought-responsive TFs have not been reported previously in a woody species, some of their orthologs in other species have been suggested or demonstrated to play roles in drought response and tolerance (Nakashima et al., 2014).

ANAC002/ATAF1, *ANAC019*, *ANAC055*, *ANAC072/RD26*, and *GBF3* are so far the only ABRE-containing TFs with validated roles in enhancing drought tolerance in transgenic Arabidopsis (Fujita et al., 2004, 2005; Tran et al., 2004; Wu et al., 2009; Hickman et al., 2013; Ramegowda et al., 2017). Sequences of *ANAC019* and *ANAC055* are absent from the *P. trichocarpa* genome, and the *GBF3* ortholog (Potri.002G167100) also was not included in our ABRE-containing TF lists (Supplemental Data Sets 4 and 5) because its transcript levels were not affected by 5- or 7-d drought treatments (Supplemental Data Set 6). Therefore, we focused on identifying orthologs of *ANAC002/ATAF1* and *ANAC072/RD26* in *P. trichocarpa*.

ANAC002/ATAF1 (Wu et al., 2009; Hu et al., 2010) has three *P. trichocarpa* orthologs with high protein sequence identity, *PtrNAC005* (Potri.005G069500), *PtrNAC006* (Potri.002G081000), and *PtrNAC007* (Potri.007G099400), and *ANAC072/RD26* (Tran et al., 2004; Hu et al., 2010) has two, *PtrNAC118* (Potri.011G123300) and *PtrNAC120* (Potri.001G404100) (Supplemental Figure 6 and Supplemental Data Sets 4 and 5). All these *PtrNAC* genes were highly induced by drought, showing 15- to 400-fold increases in transcript levels determined by reverse transcription quantitative PCR (RT-qPCR; Figure 2A). This suggested that these *PtrNAC* genes are strong positive regulators in the ABA-mediated drought signaling pathway, similar to *ANAC002/ATAF1* and *ANAC072/RD26* (Tran et al., 2004; Wu et al., 2009).

The five *PtrNAC* genes have one or multiple ABRE motifs in their promoters (2 kb upstream of the TSS; Figure 2B). We used ChIP with quantitative PCR (ChIP-qPCR) to analyze the influence of drought stress on H3K9ac levels in the ABRE motif regions of the promoters of these five *PtrNAC* genes. Both ChIP-qPCR (Figure 2C) and ChIP-seq (Supplemental Table 1) data consistently demonstrated that, as the duration of drought treatment increased, H3K9ac enrichment increased progressively in all the identified ABRE motif regions of the five *PtrNAC* promoters (Figure 2C). The progressive H3K9ac enrichment with drought severity implied that ABRE motifs are significant contributors to the regulation of *PtrNAC* expression in response to drought stress.

We then investigated whether the outcome of this regulation of *PtrNAC* expression induces drought tolerance. To do this, we aimed to overexpress these *PtrNAC* genes in *P. trichocarpa* and test the transgenic plants for drought response and tolerance. The five *PtrNAC* genes belong to three subgroups, with *PtrNAC006* as the sole member of its group, *PtrNAC005* and *PtrNAC007* as homologous members of one subgroup, and *PtrNAC118* and *PtrNAC120* as homologs in another subgroup (Supplemental Figure 6). From each subgroup, we selected the most highly drought-inducible member (Figure 2A; i.e., *PtrNAC006*, *PtrNAC007*, and *PtrNAC120*) for transgenic study.

Overexpressing *PtrNAC* Genes Improves Drought Tolerance of *P. trichocarpa*

We overexpressed *PtrNAC006* (Supplemental Figure 7), *PtrNAC007*, and *PtrNAC120* individually in *P. trichocarpa* under the control of a CaMV 35S promoter. From the plants containing each transgene construct, we selected the line with the highest transgene transcript level (Supplemental Figure 8A). These overexpression transgenics, named *OE-PtrNAC006*, *OE-PtrNAC007*, and *OE-PtrNAC120*, were multiplied along with the wild type and maintained in a walk-in growth chamber (see Methods) for further analysis. Three-month-old clonal copies of the wild-type and *OE-PtrNAC* plants were used for drought experiments, with a set of these copies being well watered and another set of these copies (at least 12 for the wild type and for each transgenic type) grown without watering for 12 d. Our screening experiments (Supplemental Figure 1) demonstrated that 12-d drought was lethal to 3-month-old wild-type *P. trichocarpa* plants; therefore, this was used for drought tolerance (survival rate) tests. All *OE-PtrNAC* transgenics exhibited drought tolerance, which was particularly strong for *OE-PtrNAC006* plants, while wild-type plants showed severe wilting symptoms (Figure 3A). The growth of *OE-PtrNAC006* transgenics was reduced (Figure 3B), but they wilted to a much lesser extent than the wild type and the other transgenic types (Figure 3A).

After the drought treatment, all plants were rehydrated for 3 d to estimate their survival rates. Most of the wild-type plants did not recover, giving only a 13% survival rate (Figures 3A and 3C). By contrast, all transgenics recovered rapidly (Figure 3A), with

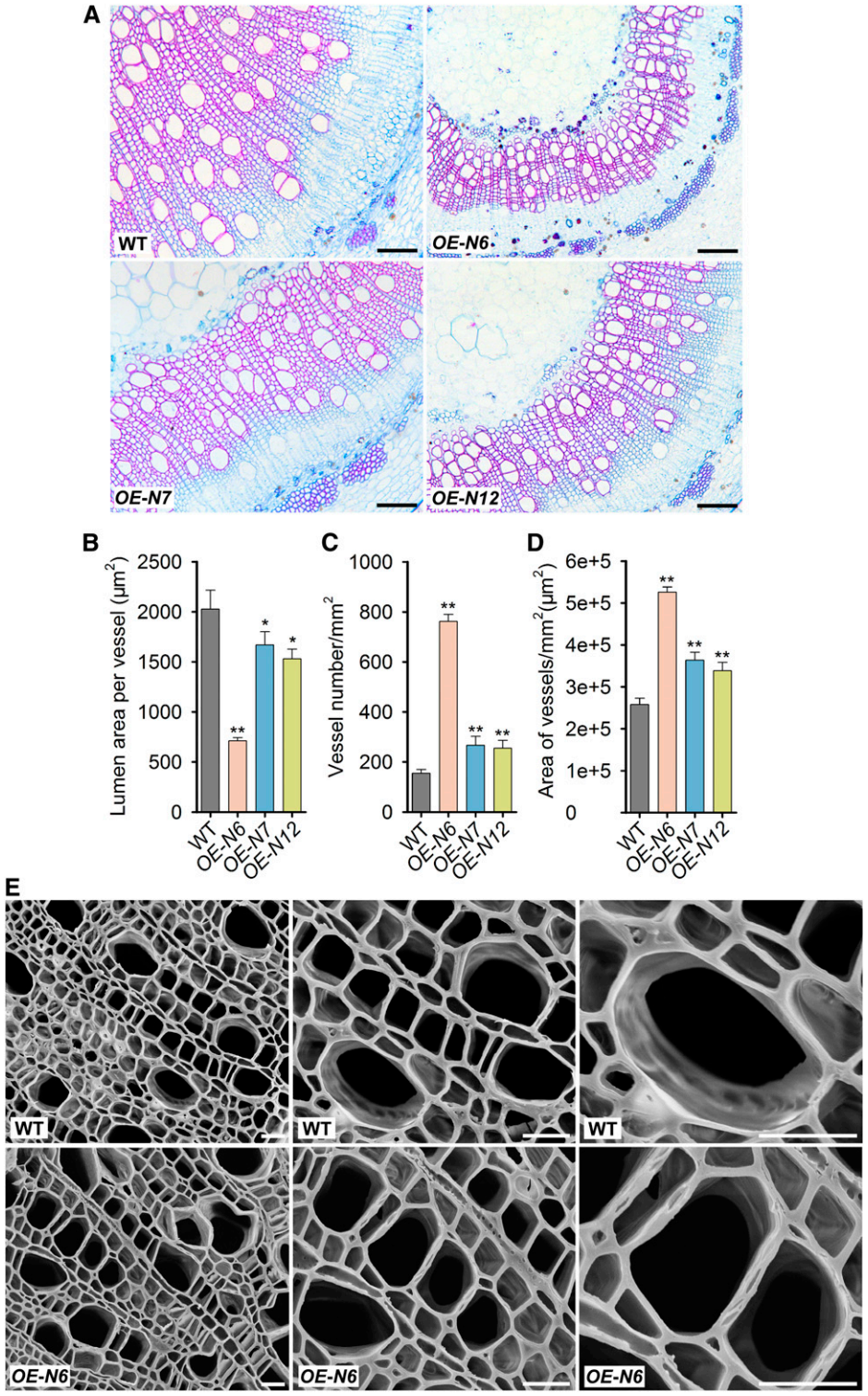

Figure 4. Overexpressing *PtrNAC* Genes Affects the Size and Number of Vessels in Xylem Tissue of *P. trichocarpa*.

(A) Stem cross sections of wild-type and *OE-PtrNAC* transgenic plants with the 10th internode. Bars = 200 μm.
(B) to **(D)** Statistical analysis of mean lumen area of individual vessels (μm^2) **(B),** number of vessels per cross-sectional area (mm^2) **(C)**, and area of vessels (μm^2) per cross-sectional area (mm^2) **(D)** using vessel cells from **(A)**. Error bars represent 1 SE of three independent replicates with at least 200 vessel cells for each

survival rates of ~76% for *OE-PtrNAC006*, ~56% for *OE-PtrNAC007*, and ~39% for *OE-PtrNAC120* (Figure 3C). The recovered transgenics were maintained in a growth room, where they began to exhibit similar growth and development to their well-watered clonal copies, whereas the drought-stressed wild-type plants grew more slowly than their well-watered controls (Supplemental Figure 8B). Therefore, *OE-PtrNAC* transgenics were both drought tolerant and resilient, particularly the *OE-PtrNAC006* plants.

We next examined the effect of *PtrNAC* gene overexpression on alterations in physiology that may contribute to drought survival. Higher stem xylem water potential can prevent drought-induced hydraulic failure and enhance drought resistance (Choat et al., 2012). Consistent with the visible phenotypes, *OE-PtrNAC* plants had higher stem xylem water potential under drought stress (Figure 3D) than did wild-type plants. We then analyzed the morphology of stem xylem cells. The structure and size of stem xylem vessels, the conducting cells, are key factors affecting water transport in plants and are important determinants of drought tolerance (Fisher et al., 2007). The stem xylem vessels in all *OE-PtrNAC* plants, *OE-PtrNAC006* in particular, were smaller than those in wild-type plants (Figures 4A, 4B, and 4E; data for *OE-PtrNAC007* and *OE-PtrNAC120* are given in Supplemental Figure 9). The vessel number per unit of area in all *OE-PtrNAC* plants was much greater than that in wild-type plants; a more than 4-fold increase in number was observed in *OE-PtrNAC006* (Figure 4C). Consequently, the area of vessels (void area) in the transverse section of the woody stem was increased significantly in all *OE-PtrNAC* plants (Figure 4D). The increase may contribute to more effective water transport in plants.

Our results indicate that *PtrNAC006*, *PtrNAC007*, and *PtrNAC120* are effector genes that transduce key physiological alterations conducive to drought tolerance and resilience. Therefore, we focused on these genes to investigate whether there is interplay between H3K9ac and AREB1-type TFs and how such an interplay regulates the expression of effector genes for drought tolerance in plants. To do this, we first examined AREB1 TF homologs in *P. trichocarpa* and their responses to drought.

PtrAREB1-2 Activates the Transcription of the Three *PtrNAC* Genes and Binds Directly to the ABRE Motifs in Their Promoters

The AREB1 TF binds to the ABRE motif in promoters of drought-responsive genes to activate the expression of these genes for drought tolerance (Fujita et al., 2011). Transgenic Arabidopsis overexpressing *AREB1* exhibits enhanced drought tolerance (Fujita et al., 2005, 2011). We identified four *AREB1* homologs in *P. trichocarpa*: *PtrAREB1-1* (Potri.001G371300), *PtrAREB1-2* (Potri.002G125400), *PtrAREB1-3* (Potri.009G101200), and *PtrAREB1-4* (Potri.014G028200). However, the *PtrAREB1-1* transcript could not be detected in RNA-seq of SDX, with and without drought treatment. Both RNA-seq and RT-qPCR analyses revealed that the remaining three *PtrAREB1* genes (*PtrAREB1-2*, *-3*, and *-4*) were readily detectable in SDX at ND and highly and similarly induced after D5 or D7 drought treatments (Figure 5A; Supplemental Data Set 6). Among these three, *PtrAREB1-2* showed the highest protein sequence identity (Supplemental Figure 10) to the Arabidopsis *AREB1* gene, which mediates a strong drought tolerance in Arabidopsis (Fujita et al., 2005). Thus, we focused on *PtrAREB1-2* to test whether the AREB1 TF coordinates ABRE motif-induced H3K9ac enrichment to regulate the expression of drought-tolerance effector genes, such as *PtrNAC006*.

In Arabidopsis, AREB1 is a transcriptional activator of ABRE-mediated genes (Fujita et al., 2005). Full activation of AREB1 requires ABA (Fujita et al., 2005; Yoshida et al., 2010), and activation activity is regulated by the ABA-dependent phosphorylation of multiple sites within the conserved domains of AREB1 (Furihata et al., 2006). We tested whether PtrAREB1-2 can activate the expression of the three *PtrNAC* effector genes, the ABRE-mediated genes, in *P. trichocarpa*. We overexpressed *PtrAREB1-2* in *P. trichocarpa* SDX protoplasts (Lin et al., 2013, 2014) to identify transregulation targets of TFs in vivo. RT-qPCR analysis demonstrated a modest effect of *PtrAREB1-2* overexpression on the expression of the *PtrNAC* effector genes (Supplemental Figure 11). However, in the presence of external ABA, overexpression of *PtrAREB1-2* induced significant increases in transcript levels of the three *PtrNAC* genes (Figure 5B). These results suggested that *PtrNAC006*, *PtrNAC007*, and *PtrNAC120* are *PtrAREB1-2*-mediated positive regulators in the ABA-dependent signaling pathway for drought tolerance. This mediation further suggests that PtrAREB1-2 binds directly to ABRE motifs in the promoters of *PtrNAC006*, *PtrNAC007*, and *PtrNAC120*, enabling gene transactivation.

To determine whether PtrAREB1-2 binds directly to ABRE motifs in the promoters of *PtrNAC* genes, anti-GFP antibody ChIP was performed using SDX protoplasts constitutively expressing a PtrAREB1-2-GFP fusion. We isolated SDX protoplasts and transfected a portion of the protoplasts with a plasmid DNA (pUC19-$35S_{pro}$-*PtrAREB1-2-GFP*) for overexpressing PtrAREB1-2-GFP. Another portion of the SDX protoplasts was transfected with a pUC19-$35S_{pro}$-*sGFP* plasmid as a mock control. After 12 h, chromatin was isolated from the transfected protoplasts for ChIP and qPCR analyses. We detected 3- to 6-fold enrichment of ABRE motif sequences from the three *PtrNAC* genes (Figure 5C), confirming that PtrAREB1-2 binds directly to ABRE motifs in the promoters of these *NAC* genes in *P. trichocarpa*. We also used an electrophoretic mobility shift assay (EMSA) to test for the direct binding of PtrAREB1-2 to ABRE motifs in promoters of *PtrNACs*. Retardation of DNA probe mobility and competition analyses demonstrated that PtrAREB1-2 could bind directly to the ABRE

Figure 4. (continued).

genotype in each replicate, and asterisks indicate significant differences between the transgenics harboring each gene construct and wild-type plants (*, $P < 0.05$ and **, $P < 0.01$, Student's *t* test).

(E) Scanning electron micrographs of wild-type and *OE-PtrNAC006* transgenic plants with the 10th internode imaged at ×500, ×1000, and ×2000 magnification. Bars = 20 μm.

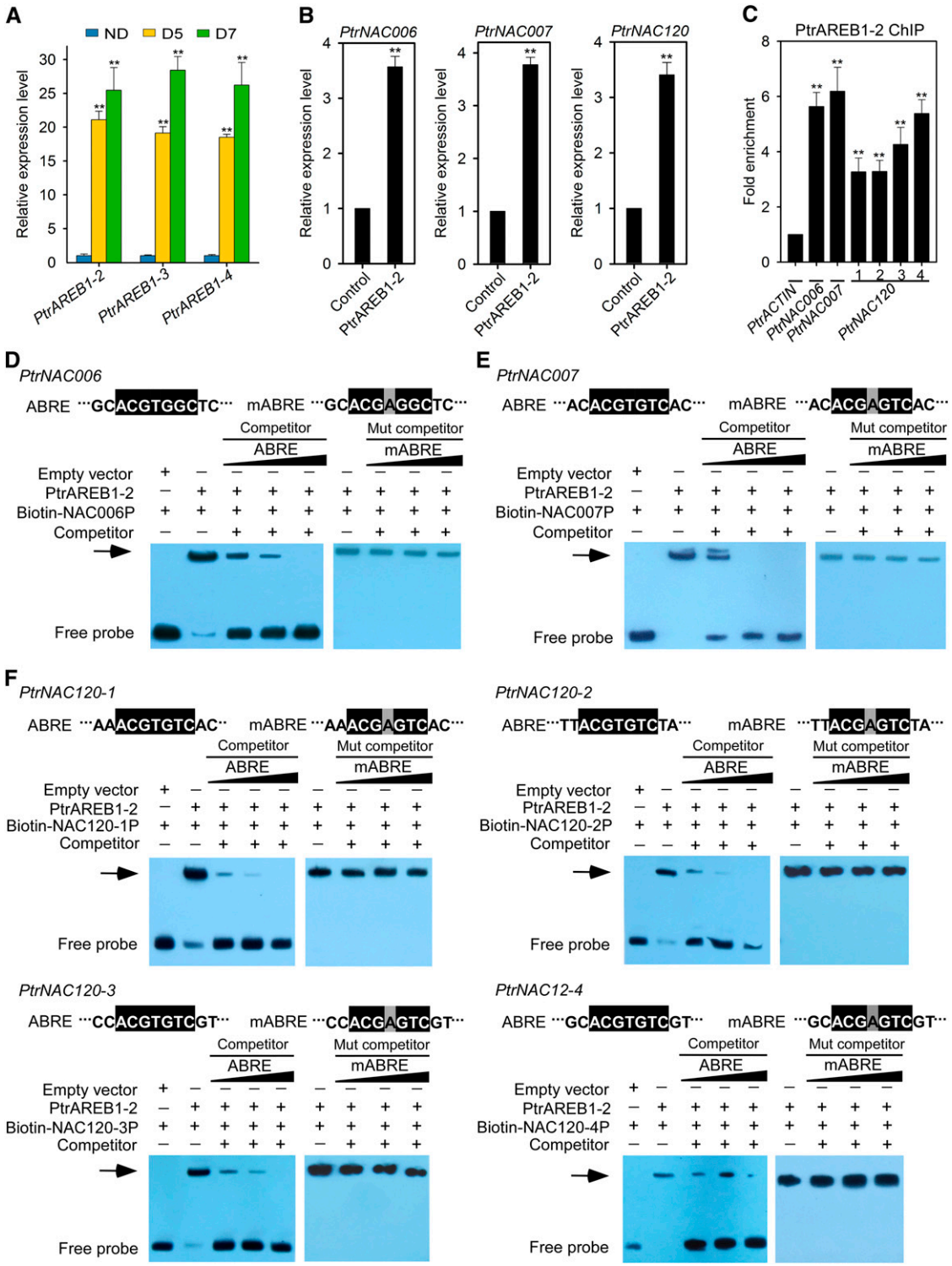

Figure 5. PtrAREB1-2 Activates the Transcription of *PtrNAC* Genes and Binds Directly to the ABRE Motifs in Their Promoters.

(A) Expression patterns of *PtrAREB1-2*, *PtrAREB1-3*, and *PtrAREB1-4* genes in response to drought stress detected by RT-qPCR. Expression was highly induced by drought treatment. Error bars indicate 1 SE of three biological replicates from independent pools of *P. trichocarpa* SDX tissues. Asterisks indicate significant differences between control (ND) and drought-treated (D5 and D7) samples for each gene (**, $P < 0.01$, Student's *t* test).

motifs in promoters of the three *PtrNAC* genes (Figures 5D to 5F). Furthermore, EMSA competition analyses with ABRE competitors carrying a single nucleotide mutation confirmed that the core ACGTGG/TC sequence is essential for PtrAREB1-2 binding to ABRE motifs (Figures 5D to 5F). We next investigated how such binding mediates the increased H3K9ac (Figure 2C) to regulate the expression of *NAC* genes (Figure 2A).

AREB1 TFs Interact with the HAT Complex ADA2b-GCN5

TFs typically interact with transcriptional coactivators for binding to the specific regions of their target gene promoters for transcriptional regulation (Stockinger et al., 2001; Mao et al., 2006; Weiste and Dröge-Laser, 2014; Zhou et al., 2017). The SAGA (Spt-Ada-Gcn5 acetyltransferase) complex is a highly conserved transcriptional coactivator that is involved in the transcription of nearly all active genes in yeast and plants (Koutelou et al., 2010; Bonnet et al., 2014; Zhou et al., 2017). We hypothesized that an ADA2b-GCN5 HAT complex (Vlachonasios et al., 2003) may be recruited to the promoters of drought-tolerance effector genes, such as the *PtrNAC* genes, by AREB1 to elevate the acetylation of H3K9, leading to the activation of these effector genes. To test this hypothesis, we first surveyed the *P. trichocarpa* genome and found an ADA2b-like protein (PtrADA2b, Potri.004G135400) with a sequence similar to that of Arabidopsis ADA2b (47% protein sequence identity). Furthermore, *PtrADA2b* was induced by drought stress based on our RT-qPCR (Figure 6A) and RNA-seq (Supplemental Data Set 6) analyses. We then cloned *PtrADA2b* cDNAs to study their transcriptional functions. The *PtrADA2b* gene has five exons and four introns, encoding cDNAs of ~0.5 kb. The cDNAs were PCR amplified from SDX of *P. trichocarpa*, and three products of ~0.5, ~0.8, and ~1.0 kb were obtained (Supplemental Figure 12A). Sequence analysis of the three products showed that pre-mRNAs from the *PtrADA2b* gene underwent alternative splicing events in the fourth exon and third intron, generating three splice variants (*PtrADA2b-1*, *PtrADA2b-2*, and *PtrADA2b-3*; Supplemental Figure 12B). Among the three splice variants of *PtrADA2b*, *PtrADA2b-3* showed the highest protein sequence identity to the Arabidopsis *ADA2b* gene. Therefore, we focused on *PtrADA2b-3* for further study.

We also found two GCN5 homologs, *PtrGCN5-1* (Potri.002G045900) and *PtrGCN5-2* (Potri.005G217400), in the *P. trichocarpa* genome (Supplemental Data Set 6). The two homologs share 84% protein sequence identity. Although *PtrGCN5-1* was not a DEG in RNA-seq (Supplemental Data Set 6), RT-qPCR results demonstrated that *PtrGCN5-1* was drought inducible and expressed abundantly in xylem tissue (Figure 6B). However, *PtrGCN5-2* was expressed at very low levels under both well-watered and drought conditions (Figure 6B). We selected *PtrGCN5-1* together with *PtrADA2b-3* to test our hypothesis that an ADA2b-GCN5 HAT complex can be recruited by AREB1 for hyperacetylating H3K9 to activate the ABRE-mediated genes. Therefore, in *P. trichocarpa*, there should be a ternary protein complex, PtrADA2b-PtrGCN5-PtrAREB1, that binds to ABRE motifs of *PtrNAC* genes, such as *PtrNAC006*, to elevate their H3K9ac.

Having already demonstrated that PtrAREB1 binds directly to the ABRE motifs of *PtrNAC006*, *PtrNAC007*, and *PtrNAC120* (Figures 5C to 5F), we next tested the potential interactions among PtrADA2b-3, PtrGCN5-1, and PtrAREB1-2 in vitro and in vivo. We first tested the pairwise interaction between PtrADA2b-3 and PtrGCN5-1. Pull-down assays using *Escherichia coli*-produced PtrGCN5-1:6×His-tag and PtrADA2b-3:S-tag, or PtrGCN5-1:6×His-tag and GFP:S-tag, fusion proteins showed that PtrADA2b-3:S-tag, but not GFP:S-tag, was retained by the PtrGCN5-1:6×His protein, indicating that PtrGCN5-1 interacts with PtrADA2b-3 (Figure 6C). We then tested pairwise interactions between PtrADA2b-3 and PtrAREB1-2 and between PtrAREB1-2 and PtrGCN5-1. In vitro pull down demonstrated interactions between the S-tagged PtrADA2b-3 and the His-tagged PtrAREB1-2 (Figure 6D) and between the S-tagged PtrAREB1-2 and the His-tagged PtrGCN5-1 (Figure 6E). These pairwise (PtrADA2b-3:PtrGCN5-1, PtrADA2b-3:PtrAREB1-2, and PtrAREB1-2:PtrGCN5-1) interactions suggest the involvement of ternary protein complexes made from PtrADA2b, PtrGCN5, and PtrAREB1. We then performed bimolecular fluorescence complementation (BiFC) assays to confirm the presence of these pairwise interactions in vivo using *P. trichocarpa* SDX protoplasts.

PtrADA2b-3:YFP^N, where PtrADA2b-3 was fused to the N terminus of YFP (amino acids 1–174), and PtrGCN5-1:YFP^C, where PtrGCN5-1 was fused to the C terminus of YFP (amino acids 175–239), were coexpressed together with the H2A-1:mCherry nuclear marker in SDX protoplasts. The presence of the two fusion proteins reconstituted YFP signals, which were colocalized with

Figure 5. (continued).

(B) RT-qPCR to detect the transcript abundance of *PtrNAC006*, *PtrNAC007*, and *PtrNAC120* in SDX protoplasts overexpressing *GFP* (Control) or *PtrAREB1-2* in the presence of external 50 μM ABA. Control values were set as 1. Error bars indicate 1 SE of three biological replicates (three independent batches of SDX protoplast transfections). Asterisks indicate significant differences for each gene between control protoplasts and those overexpressing *PtrAREB1-2* samples for each gene (**, $P < 0.01$, Student's *t* test).

(C) PtrAREB1-2 ChIP assays showing that PtrAREB1-2 binds directly to the promoters of *PtrNAC* genes. *P. trichocarpa* SDX protoplasts overexpressing *PtrAREB1-2-GFP* or *GFP* (control) were used for the ChIP assay with anti-GFP antibody, and the precipitated DNA was quantified by qPCR. Enrichment of DNA was calculated as the ratio between $35S_{pro}$:*PtrAREB1-2-GFP* and $35S_{pro}$:*GFP* (control), normalized to that of the *PtrACTIN* gene. Numbers indicate ABRE motif sites in *PtrNAC120*. Error bars represent 1 SE of three biological replicates (three independent batches of SDX protoplast transfections). Asterisks indicate significant differences between the control fragment (*PtrACTIN*) and each fragment containing an ABRE motif (**, $P < 0.01$, Student's *t* test).

(D) to **(F)** Nucleotide sequences of the wild-type ABRE and a mutated ABRE motif (mABRE) (top panels). Core sequences are shaded in black, and the mutated nucleotide is shaded in gray. EMSA analysis of PtrAREB1-2 binding to ABRE motifs in *PtrNAC006* **(D)**, *PtrNAC007* **(E)**, and *PtrNAC120* **(F)** promoters is shown in the bottom panels. The arrows show the shifted band representing the protein-DNA complex. *PtrNAC006* **(D)**, *PtrNAC007* **(E)**, and *PtrNAC120* **(F)** promoter fragments were labeled with biotin. Fragments without biotin labeling were used as competitors. Wild-type or mutated ABRE competitors were used in a molar excess of 50×, 100×, or 150×.

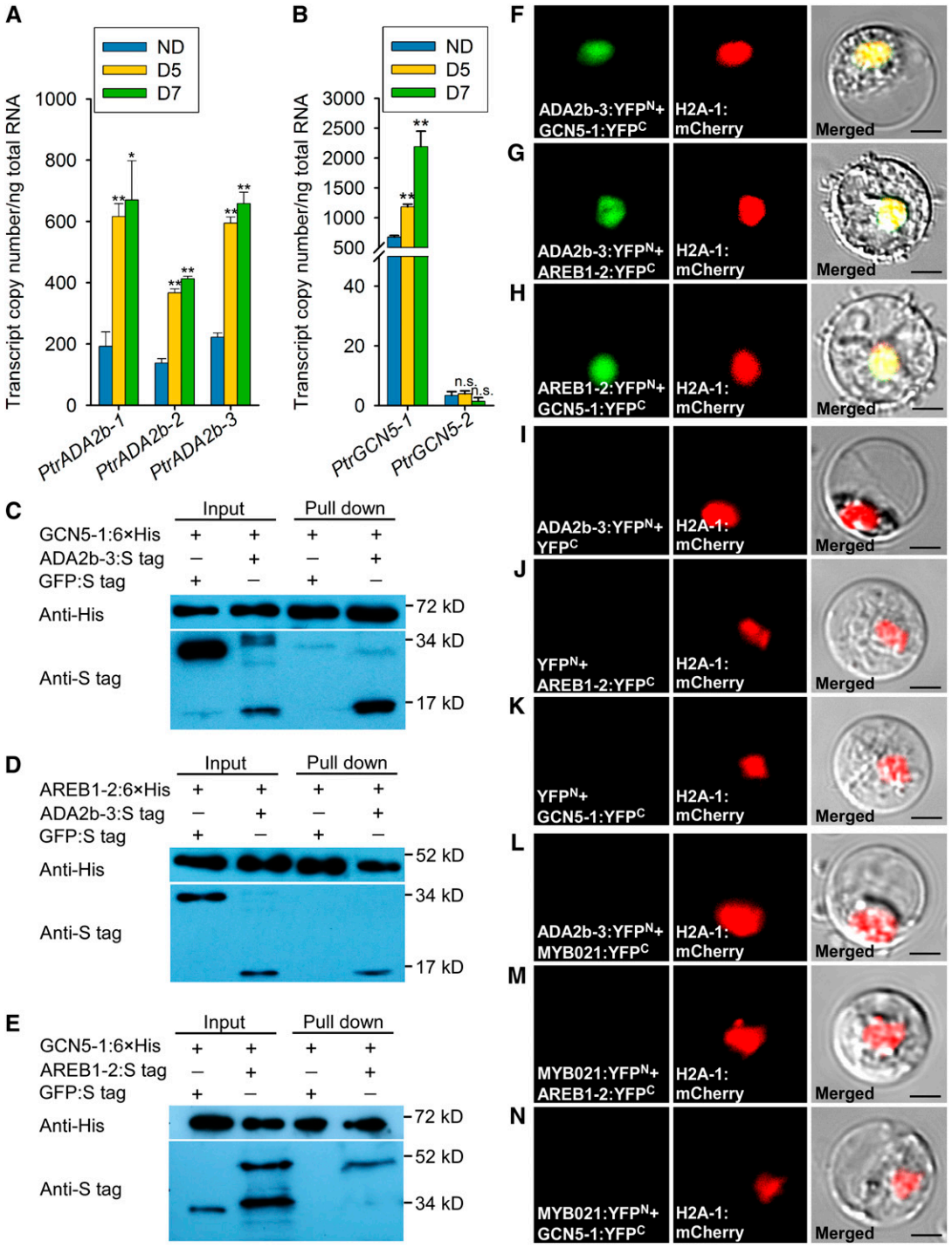

Figure 6. PtrAREB1-2 Interacts with the HAT Complex PtrADA2b-3:PtrGCN5-1.

(A) and **(B)** Abundance of alternatively spliced transcripts of *PtrADA2b-1*, *PtrADA2b-2*, and *PtrADA2b-3* **(A)** as well as *PtrGCN5-1* and *PtrGCN5-2* **(B)** determined by RT-qPCR in the xylem of *P. trichocarpa* under well-watered and drought conditions. Error bars indicate 1 SE of three biological replicates in **(A)** and six biological replicates in **(B)** from independent pools of *P. trichocarpa* SDX tissues. Asterisks indicate significant differences between control (ND) and drought-treated (D5 and D7) samples for each gene (*, $P < 0.05$ and **, $P < 0.01$, Student's *t* test), and n.s. denotes no significant difference.

(C) to **(E)** Interactions of PtrADA2b-3, PtrGCN5-1, and PtrAREB1-2 with each other determined by pull-down assays. His-tagged PtrGCN5-1 and PtrAREB1-2 as well as S-tagged PtrADA2b-3 and PtrAREB1-2 purified from *E. coli* were used for pull-down assays, and GFP was used as a negative control.

H2A-1:mCherry exclusively in the nucleus, confirming that PtrADA2b-3 interacts with PtrGCN5-1, forming dimers in vivo (Figure 6F; Supplemental Figures 13A and 13J). Nucleus-localized YFP signals also were observed for moieties representing dimers of PtrADA2b-3 and PtrAREB1-2 (Figure 6G; Supplemental Figures 13B and 13K) and of PtrAREB1-2 and PtrGCN5-1 (Figure 6H; Supplemental Figures 13C and 13L). Empty plasmids and PtrMYB021, an unrelated TF expressed in the nucleus (Li et al., 2012), were used as negative controls. Cotransfection of each protein of interest with empty plasmid did not yield any YFP signal (Figures 6I to 6K; Supplemental Figures 13D to 13F and 13M to 13O). Coexpression of the PtrADA2b-3:YFP^N fusion and PtrMYB021:YFP^C (Figure 6L; Supplemental Figures 13G and 13P), of PtrMYB021:YFP^N and PtrAREB1-2:YFP^C (Figure 6M; Supplemental Figures 13H and 13Q), or of PtrMYB021:YFP^N and PtrGCN5-1:YFP^C (Figure 6N; Supplemental Figures 13I and 13R) with H2A-1:mCherry resulted in the detection of only H2A-1:mCherry signals in the nucleus, demonstrating the interaction specificity between the paired proteins tested. The observed YFP signals (Figures 6F to 6H; Supplemental Figures 13A to 13C and 13J to 13L), therefore, were the consequence of dimerization of the paired proteins tested. These results are consistent with the in vitro evidence (Figures 6C to 6E) suggesting ternary protein complexes involving PtrADA2b-3, PtrGCN5-1, and PtrAREB1-2.

PtrADA2b-3 and PtrGCN5-1 Together Enhance the PtrAREB1-Mediated Transcriptional Activation of *PtrNAC* Genes by Increasing H3K9ac Level and RNA Pol II Recruitment at Their Promoters

The in vitro and in vivo protein interaction assays and ChIP-qPCR validated our hypothesis that PtrADA2b-3, PtrGCN5-1, and PtrAREB1-2 form dimeric or ternary protein complexes (Figures 6C to 6N; Supplemental Figures 13A to 13R) for binding to ABRE motifs in promoters of the *PtrNAC* genes (Figure 5C). Binding is through the complex's PtrAREB1-2 member, creating a *PtrNAC* gene-specific HAT system to mediate enhanced H3K9ac of *NAC* genes for their elevated expression. However, we demonstrated that PtrAREB1-2 alone (in the presence of external ABA) can mediate the elevated expression of the three *PtrNAC* genes (Figure 5B). Therefore, we tested whether the formation of dimeric or trimeric protein complexes is necessary to enhance the PtrAREB1-2-mediated transcriptional activation of the three *PtrNAC* genes. We overexpressed (1) *PtrAREB1-2*, (2) *PtrGCN5-1*, (3) *PtrADA2b-3*, (4) the *PtrAREB1-2*:*PtrGCN5-1* fusion gene, (5) the *PtrAREB1-2*:*PtrADA2b-3* fusion, (6) the *PtrADA2b-3*:*PtrGCN5-1* fusion, and (7) the *PtrAREB1-2*:*PtrADA2b-3*:*PtrGCN5-1* fusion, individually, in *P. trichocarpa* SDX protoplasts and compared the overexpression effects on the transcript levels of the three *PtrNAC* genes using *GFP* expression as a control. ABA was applied when the transfected protoplasts were incubated.

As already demonstrated (Figure 5B), in the presence of external ABA, overexpression of PtrAREB1-2 alone effectively activated the expression of the three *NAC* genes (Figure 7A). Other individual (PtrGCN5-1 and PtrADA2b-3) or dimeric (PtrAREB1-2:PtrGCN5-1, PtrAREB1-2:PtrADA2b-3, and PtrADA2b-3:PtrGCN5-1) proteins also could activate the three *NAC* genes, but with similar or lower activation efficiency to PtrAREB1-2 alone (Figure 7A). Therefore, PtrAREB1-2 alone through its binding to the ABRE motif establishes a basic transregulation system for activating *NAC* genes. The dimerization of PtrGCN5-1 or PtrADA2b-3 with PtrAREB1-2 is not necessary for this basic transregulation system because such dimers had no effect on *NAC* gene activation mediated by PtrAREB1-2 alone (Figure 7A).

By contrast, the ternary complex, PtrAREB1-2:PtrADA2b-3:PtrGCN5-1, strongly induced the activation of the three *NAC* genes, nearly doubling the activation levels mediated by PtrAREB1-2 alone (Figure 7A). Based on our RNA-seq and ChIP-seq data, we selected five drought-responsive *PtrNAC* genes without ABRE motifs in their promoters as negative controls. Two (*PtrNAC071* [Potri.019G099900] and *PtrNAC091* [Potri.019G099800]) of the five have neither an ABRE motif nor an H3K9ac mark in their promoters. The remaining three (*PtrNAC047* [Potri.013G054000], *PtrNAC083* [Potri.017G063300], and *PtrNAC100* [Potri.017G086200]) also have no ABRE motif but do have H3K9ac marks in their promoters. Members of the ternary complex, individually or in any dimeric or trimeric combination, could not activate any of these five negative control genes (Figure 7A).

We also repeated the SDX protoplast overexpression experiments in the absence of external ABA for all seven transgenes described above and found that the transregulation effects were nearly identical to those in the presence of ABA, but the activation of the three *NAC* genes was significantly lower (Supplemental Figure 14). We concluded that PtrADA2b and PtrGCN5 together could enhance the PtrAREB1-mediated transcriptional activation of *PtrNAC* genes. These results also support our hypothesis that a PtrADA2b-PtrGCN5 HAT complex is recruited by AREB1 to *PtrNAC* gene promoters that must have the ABRE motif, elevating their H3K9ac level and leading to the activation of these *NAC* genes. We next tested whether the enhancement of the PtrAREB1-mediated *PtrNAC* gene activation is a result of increasing H3K9ac levels at their promoters.

The complete set of monomeric and oligomeric proteins used to verify their effects on *PtrNAC* gene activation (Figure 7A) also was used in SDX protoplast-based ChIP-qPCR to test their influence on the enrichment of H3K9ac in promoters of the *PtrNAC* genes that they bind to. Therefore, SDX protoplasts were transfected with (1) $35S_{pro}$:*PtrAREB1-2*, (2) $35S_{pro}$:

Figure 6. (continued).

(F) to **(N)** BiFC assays in *P. trichocarpa* SDX protoplasts showing that PtrADA2b-3, PtrGCN5-1, and PtrAREB1-2 proteins interact with each other in the nucleus (**[F]** to **[H]**). Cotransfection of each protein of interest with an empty plasmid served as a control (**[I]** to **[K]**). PtrMYB021, an unrelated TF expressed in the nucleus (Li et al., 2012), was used as another negative control (**[L]** to **[N]**). Neither negative control gave any YFP signal. Green shows the YFP signals from protein interaction, red indicates the nuclear marker H2A-1:mCherry, and yellow represents the merged signals from YFP and mCherry. Images from two other biological replicates are shown in Supplemental Figure 13. Bars = 10 μm.

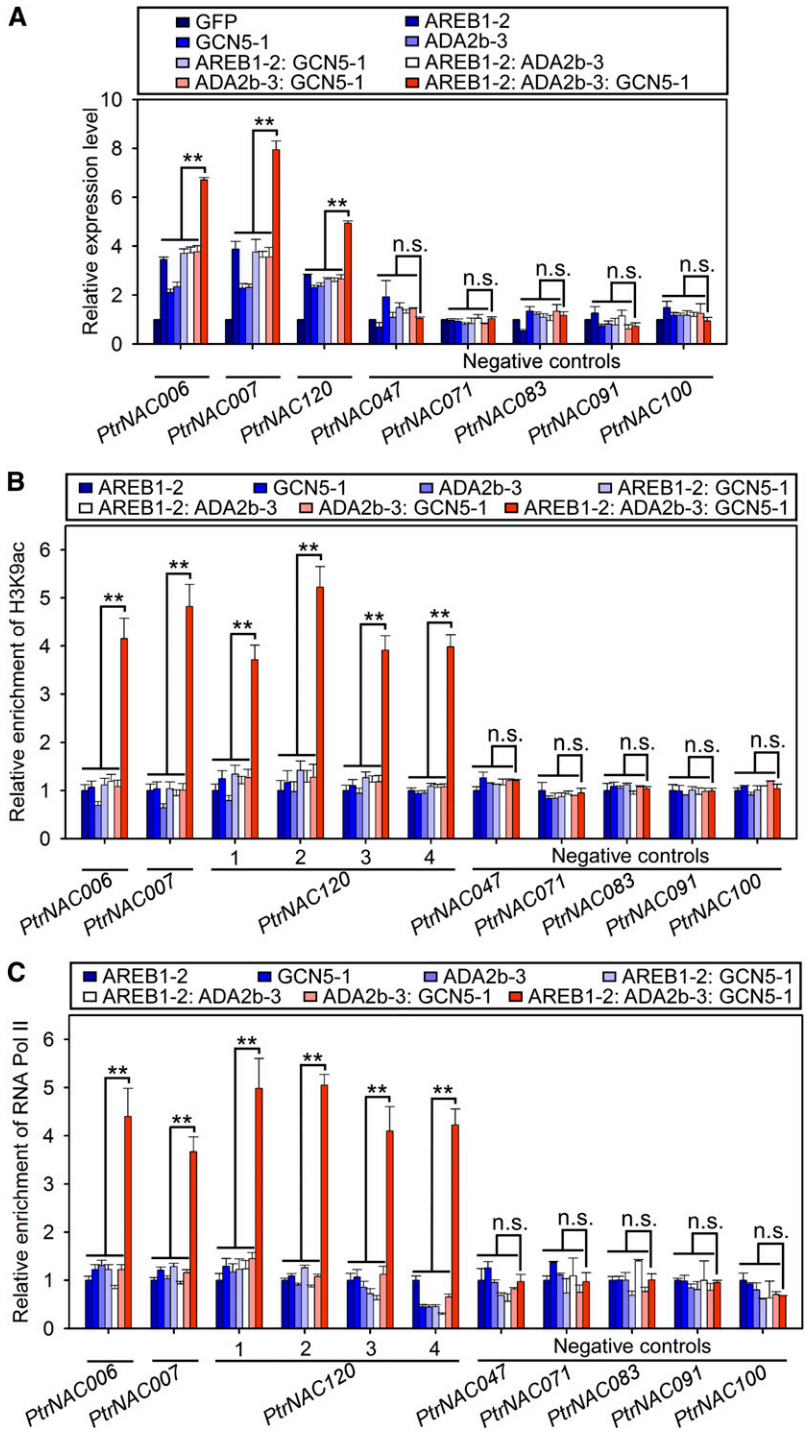

Figure 7. PtrADA2b-3 and PtrGCN5-1 Together Enhance PtrAREB1-2-Mediated Transcriptional Activation of *PtrNAC* Genes by Increasing H3K9ac Level and RNA Pol II Recruitment at Their Promoters.

(A) RT-qPCR detection of *PtrNAC006*, *PtrNAC007*, and *PtrNAC120* transcripts in *P. trichocarpa* SDX protoplasts overexpressing *GFP* (control), *PtrAREB1-2*, *PtrGCN5-1*, *PtrADA2b-3*, *PtrAREB1-2*:*PtrGCN5-1*, *PtrAREB1-2*:*PtrADA2b-3*, *PtrADA2b-3*:*PtrGCN5-1*, or *PtrAREB1-2*:*PtrADA2b-3*:*PtrGCN5-1* in the presence of external 50 μM ABA. Five genes without ABRE motifs were used as negative controls, none of which had activated expression. The control values were set as 1. Error bars represent 1 SE of three biological replicates (three independent batches of SDX protoplast transfections). Asterisks indicate significant differences between the ternary complex and each monomeric or dimeric protein for each gene (**, $P < 0.01$, Student's *t* test), and n.s. denotes no significant difference.

PtrGCN5-1, (3) $35S_{pro}$:*PtrADA2b-3*, (4) $35S_{pro}$:*PtrAREB1-2*:*PtrGCN5-1*, (5) $35S_{pro}$:*PtrAREB1-2*:*PtrADA2b-3*, (6) $35S_{pro}$:*PtrADA2b-3*:*PtrGCN5-1*, and (7) $35S_{pro}$:*PtrAREB1-2*:*PtrADA2b-3*:*PtrGCN5-1* constructs, with $35S_{pro}$:*GFP* as the control, and assayed by anti-H3K9ac antibody ChIP following our previously described protocol (Li et al., 2014). All tested monomeric and dimeric proteins induced nearly identical levels of H3K9ac at the ABRE motif regions (Figure 2B) in the promoters of the *PtrNAC* genes (Figure 7B). This H3K9ac level was elevated drastically in the presence of the ternary protein complex derived from the $35S_{pro}$:*PtrAREB1-2*:*PtrADA2b-3*:*PtrGCN5-1* transgene (Figure 7B). None of the monomeric, dimeric, or trimeric proteins could induce any H3K9ac enrichment in promoters of the five *PtrNAC* control genes lacking the ABRE motif (Figure 7B). The results suggest that PtrAREB1-2 alone induces a basal level of H3K9ac for the transcriptional activation of the *PtrNAC* genes (Figure 7A).

Levels of H3K9ac can be augmented readily by recruiting the effective HAT complex (PtrADA2b-3:PtrGCN5-1 dimers) to PtrAREB1-2, which binds to the promoters (ABRE motifs) of *PtrNAC* genes, enhancing transcription. Because gene transcription, particularly of TF genes, also is mediated by RNA Pol II binding to the upstream promoter of the genes (Roeder, 1996), we then asked if the increase in PtrAREB1-mediated transcriptional activation of *PtrNAC* genes correlates with their enhanced RNA Pol II recruitment. We examined the occupancy of total RNA Pol II at the promoters of the three *PtrNAC* genes in SDX protoplasts transfected with the same set of seven transgene constructs plus control described above; transfected protoplasts were assayed by anti-Pol II antibody ChIP followed by qPCR.

The effects of the different transgenic proteins on the levels of RNA Pol II enrichment at promoters of the three *PtrNAC* genes were similar to those on levels of H3K9ac enrichment. PtrAREB1-2 alone binding to the *NAC* gene was accompanied by a basal level of RNA Pol II enrichment (Figure 7C), which was enhanced strongly when PtrADA2b-3:PtrGCN5-1 formed a complex with PtrAREB1-2 (Figure 7C). Again, none of the five negative control genes had enhanced RNA Pol II levels at their promoters (Figure 7C). These results suggest that the enhancement of PtrAREB1-mediated transcriptional activation of *PtrNAC* genes is a result of increasing H3K9ac level (hyperacetylation) at their promoters creating a more "open" chromatin (Norton et al., 1989; Lee et al., 1993; Kouzarides, 2007; Zentner and Henikoff, 2013), thereby facilitating a high-level accumulation of RNA Pol II.

The protoplast results demonstrated that the ternary complex PtrAREB1-2:PtrADA2b-3:PtrGCN5-1 is necessary to establish a regulatory machinery with enhanced H3K9ac and RNA Pol II enrichment to activate the expression of the three *PtrNAC* drought-tolerance effector genes (Figure 7). We then tested, in planta, the necessity of PtrAREB1-2, PtrADA2b-3, and PtrGCN5-1 and their effects on the transcriptional regulation of the *PtrNAC* genes and on drought tolerance through RNAi and knockout transgenesis.

Reduced or Deleted Expression of *PtrAREB1-2*, *PtrADA2b-3*, or *PtrGCN5-1* in *P. trichocarpa* Decreases (1) H3K9ac and RNA Pol II Enrichment on *PtrNAC* Genes, (2) the Expression of These *NAC* Genes, and (3) Plant Drought Tolerance

We first generated 13 and 8 lines of transgenic *P. trichocarpa* in which *PtrAREB1-2* and *PtrGCN5-1*, respectively, were suppressed through RNAi. From each of these transgenic types, we selected two lines with distinct levels (highest and intermediate suppression) of target gene knockdown (RNAi6-*PtrAREB1-2* and RNAi9-*PtrAREB1-2* as well as RNAi2-*PtrGCN5-1* and RNAi5-*PtrGCN5-1* in Supplemental Figure 15A). In parallel, we modified our *P. trichocarpa* genetic transformation protocol (Song et al., 2006) to allow genome editing using CRISPR-Cas9. We generated four lines of transgenic *P. trichocarpa* and identified two biallelic mutants, *ada2b-3-1* and *ada2b-3-2* (Supplemental Figure 15B), which were named KO1-*PtrADA2b-3* and KO2-*PtrADA2b-3*, respectively. These selected transgenics were propagated and maintained in a walk-in growth chamber for further characterization.

We characterized the transgenics and mutants as well as the wild type under drought stress (withholding water for 5 d). We performed RT-qPCR on transcripts of the three *PtrNAC* genes in SDX to reveal the impact of *PtrAREB1-2*, *PtrADA2b-3*, and *PtrGCN5-1* on the expression of these *NAC* genes, which were activated drastically under drought stress (Figure 2A). The activation state of these three *NAC* genes was diminished substantially if the expression of any one of the *PtrAREB1-2*, *PtrADA2b-3*, or *PtrGCN5-1* genes was reduced (Figures 8A to 8C). These results suggest that simultaneous high expression levels of *PtrAREB1-2*, *PtrADA2b-3*, and *PtrGCN5-1* are essential to activate drought-tolerant effector genes (*NAC*).

Next, we examined the effects of *PtrAREB1-2*, *PtrADA2b-3*, and *PtrGCN5-1* on the enrichment of H3K9ac at promoters of the three *PtrNAC* genes. We performed ChIP-qPCR to quantify H3K9ac enrichment using the same SDX used for the RT-qPCR experiments above. The results demonstrated that the significantly elevated H3K9ac enrichments at the promoters of the three *NAC* genes under drought stress (Figure 2C) were reduced greatly

Figure 7. (continued).

(B) and **(C)** ChIP-qPCR showing that co-overexpression of *PtrAREB1-2*, *PtrADA2b-3*, and *PtrGCN5-1* increased H3K9ac (B) and RNA Pol II (C) enrichment at the promoters of *PtrNAC006*, *PtrNAC007*, and *PtrNAC120*. SDX protoplasts overexpressing *PtrAREB1-2*, *PtrGCN5-1*, *PtrADA2b-3*, *PtrAREB1-2*:*PtrGCN5-1*, *PtrAREB1-2*:*PtrADA2b-3*, *PtrADA2b-3*:*PtrGCN5-1*, *PtrAREB1-2*:*PtrADA2b-3*:*PtrGCN5-1*, or *GFP* (control) were used for ChIP assays with anti-H3K9ac **(B)** and anti-RNA Pol II **(C)** antibodies, and the precipitated DNA was quantified by qPCR. None of the five negative control genes had enhanced H3K9ac **(B)** or RNA Pol II **(C)** levels at their promoters. Enrichment values represent the relative fold change compared with the protoplasts overexpressing *PtrAREB1-2*. Error bars indicate 1 SE of three biological replicates (three independent batches of SDX protoplast transfections). Asterisks indicate significant differences between the ternary complex and each monomeric or dimeric protein for each fragment containing the ABRE motif (**, $P < 0.01$, Student's *t* test), and n.s. denotes no significant difference.

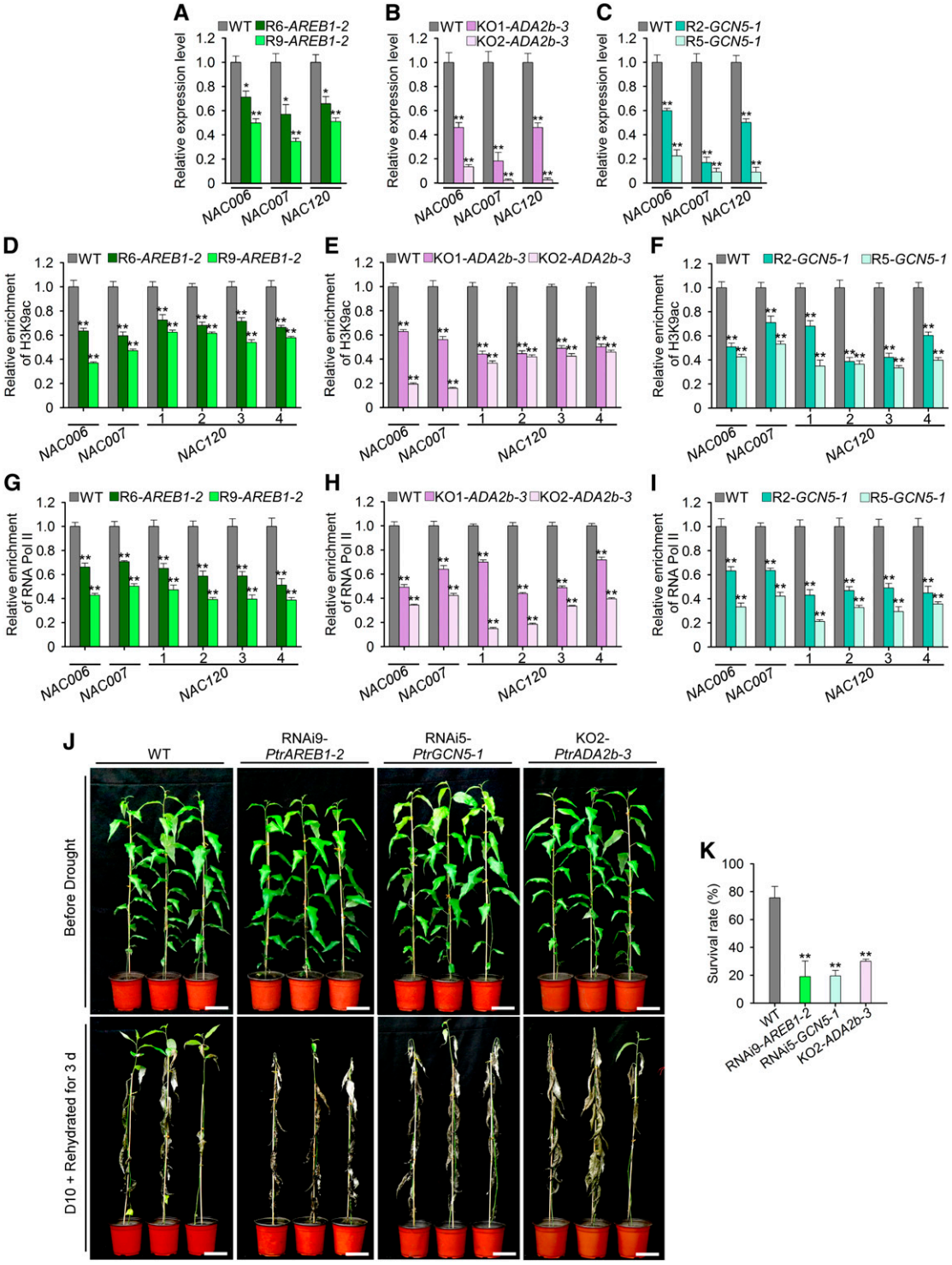

Figure 8. Reduced or Deleted Expression of *PtrAREB1-2*, *PtrADA2b-3*, or *PtrGCN5-1* in *P. trichocarpa* Decreases H3K9ac and RNA Pol II Enrichment on *PtrNAC* Genes, Expression of These *NAC* Genes, and Plant Drought Tolerance.

(A) to **(C)** RT-qPCR detection of *PtrNAC006*, *PtrNAC007*, and *PtrNAC120* transcripts in wild-type, RNAi-*PtrAREB1-2* (R6 and R9 = lines 6 and 9) **(A)**, KO-*PtrADA2b-3* (KO1 and KO2 = knockout mutants 1 and 2) **(B)**, and RNAi-*PtrGCN5-1* (R2 and R5 = lines 2 and 5) **(C)** transgenic plants following drought treatment for 5 d. Error bars indicate 1 SE of three biological replicates from independent pools of *P. trichocarpa* SDX tissues, and asterisks indicate significant differences between each transgenic line and wild-type plants for each *PtrNAC* gene (*, $P < 0.05$ and **, $P < 0.01$, Student's *t* test).

when the expression of any of the *PtrAREB1-2*, *PtrADA2b-3*, or *PtrGCN5-1* genes was reduced (Figures 8D to 8F). Similarly, using the same SDX tissue as above, the enrichment of RNA Pol II at the three *PtrNAC* gene promoters was decreased significantly in the transgenics compared with wild-type plants (Figures 8G to 8I).

Finally, we examined the transgenics and mutants for their drought tolerance and survival (Figure 8J). Preliminary examinations demonstrated that they were hypersensitive to drought and that none of them could survive the 12-d drought + 3-d rehydration cycle normally used for testing wild-type *P. trichocarpa* (Figure 3A). Therefore, we applied a milder drought (10 d) stress to these transgenic and wild-type plants. After 10 d of drought and 3 d of rehydration (see Methods), RNAi9-*PtrAREB1-2*, RNAi5-*PtrGCN5-1*, and KO2-*PtrADA2b-3* had ~19, ~20, and ~30% survival rates, respectively, contrasting with a survival rate of ~76% for wild-type plants (Figure 8K). We concluded that PtrADA2b-3, PtrGCN5-1, and PtrAREB1-2 together control the level of H3K9ac and the recruitment of RNA Pol II to promoters of drought-responsive genes (e.g., the *PtrNAC* genes), thereby conferring high expression levels of the effector gene for tolerance and survival in *P. trichocarpa*.

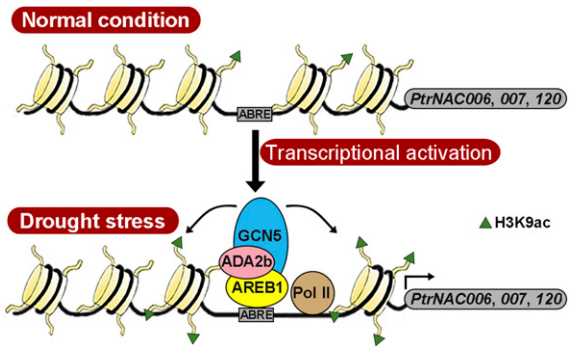

Figure 9. Proposed Model of AREB1-Mediated Histone Acetylation in the Regulation of Drought Stress-Responsive *PtrNAC* Genes.

Under drought stress conditions, the expression of the AREB1 TF is induced. AREB1 interacts with the ADA2b-GCN5 HAT complex and recruits the proteins to *PtrNAC006*, *PtrNAC007*, and *PtrNAC120* genes through binding to ABRE motifs, resulting in enhanced H3K9ac and RNA Pol II enrichment for activating the expression of the *PtrNAC006*, *PtrNAC007*, and *PtrNAC120* genes.

DISCUSSION

In this study, we reported on a regulatory system involving the coordinated regulation of H3K9 acetylation and AREB1 TF functions for activating many drought-responsive genes (or drought-tolerant effector genes; Supplemental Data Sets 4 and 5), such as some *NAC* genes, for enhanced drought tolerance in *P. trichocarpa*. It has long been known that AREBs can transactivate drought-responsive genes through binding to ABRE motifs in the promoters of these target genes to induce drought tolerance (Fujita et al., 2005; Yoshida et al., 2010; Nakashima et al., 2014). It is also known that levels of H3K9ac modification increase under drought stress. What has not been clear is the type of acetylation modifiers involved and whether such modifications induce specific drought-responsive genes to confer drought tolerance. This study helps fill this important knowledge gap, allowing a fuller understanding of the regulatory mechanisms underlying a process that is critical to plant growth and adaptation.

We integrated transcriptomic and epigenomic analyses to show that drought stress affects H3K9ac modifications genome-wide in *P. trichocarpa* and that the level of H3K9ac enrichment is associated with the transcriptional activity of drought stress-responsive genes (Figures 1A and 1B; Supplemental Figure 5). Such an association includes four unique sets of genes: the hUP-gDN, hUP-gUP, hDN-gUP, and hDN-gDN gene sets (Figures 1A and 1B). Because H3K9ac is an activating mark, the hUP-gUP and hDN-gDN set of genes is most likely to represent the direct effects of differential H3K9ac enrichments on gene expression. Therefore, the analysis of the hUP-gUP and hDN-gDN gene set is a more logical data reduction approach to start with for a more focused objective. The GO term and motif enrichment search analyses of this gene set revealed that H3K9ac likely regulates drought-responsive genes through an ABA-dependent pathway (Figure 1; Supplemental Data Set 3). These analyses led to the identification of 76 key TF genes with ABRE motifs in their promoters, including 11 *NAC* homologs (Supplemental Data Sets 4 and 5). Overexpression of three of these *NAC* genes (*PtrNAC006*, *PtrNAC007*, and *PtrNAC120*) in *P. trichocarpa* resulted in much improved drought tolerance, consistent with the phenotypes of transgenic Arabidopsis and rice, where

Figure 8. (continued).

(D) to **(F)** ChIP-qPCR detection of H3K9ac at promoters of *PtrNAC* genes in wild-type, RNAi-*PtrAREB1-2* **(D)**, KO-*PtrADA2b-3* **(E)**, and RNAi-*PtrGCN5-1* **(F)** transgenic plants following drought treatment for 5 d.

(G) to **(I)** ChIP-qPCR detection of RNA Pol II enrichment at promoters of *PtrNAC* genes in wild-type, RNAi-*PtrAREB1-2* **(G)**, KO-*PtrADA2b-3* **(H)**, and RNAi-*PtrGCN5-1* **(I)** transgenic plants following drought treatment for 5 d.

ChIP assays were performed using antibodies against H3K9ac (**[D]** to **[F]**) and RNA Pol II (**[G]** to **[I]**), and the precipitated DNA was quantified by qPCR. Enrichment values represent the relative fold change compared with wild-type plants. Numbers in **(D)** to **(I)** indicate ABRE motif sites in *PtrNAC120*. Each experiment had three biological replicates showing similar results. Error bars indicate 1 SE of three technical replicates, and asterisks indicate significant differences from wild-type plants (**, $P < 0.01$, Student's *t* test).

(J) Drought-sensitive phenotypes of RNAi9-*PtrAREB1-2*, RNAi5-*PtrGCN5-1*, and KO2-*PtrADA2b-3* transgenic plants. Three-month-old plants (Before Drought, top row) were dehydrated for 10 d and then rehydrated for 3 d (D10 + Rehydrated for 3 d, bottom row). Bars = 10 cm.

(K) Statistical analysis of survival rates after drought treatment and recovery (D10 + rehydrated for 3 d). Error bars represent 1 SE of three independent experiments with at least 12 plants of each genotype in each replicate, and asterisks indicate significant differences between the transgenics of each gene construct and wild-type plants (**, $P < 0.01$, Student's *t* test).

genes with ABRE motif-containing promoters were overexpressed (Fujita et al., 2005; Barbosa et al., 2013).

In vivo ChIP, EMSA, and in vivo transactivation assays demonstrated that PtrAREB1 binds directly to ABRE motifs of *PtrNAC006*, *PtrNAC007*, and *PtrNAC120* and is a transactivator of these ABRE-mediated *NAC* genes (Figure 5). Overexpressing *PtrAREB1-2* in *P. trichocarpa* induced strong drought tolerance in trangenics, with a 100% survival rate (Supplemental Figures 16A and 16C). Therefore, either activating *PtrAREB1-2*, which enhances the expression of ABRE-mediated drought-responsive genes, or directly activating genes with ABRE motif-containing promoters induces drought tolerance in transgenic *P. trichocarpa* (Figure 3). These results suggest that plants activate either AREB1 or ABRE-mediated genes in response to drought stress to develop tolerance for survival. However, knowledge about the activation mechanism has been lacking.

We now reveal that, while binding to the ABRE motifs of drought-responsive genes (*PtrNACs*) (Figures 5B and 7A), PtrAREB1-2 recruits the SAGA-like HAT complex PtrADA2b-3:PtrGCN5-1, forming ternary protein complexes (Figures 6C to 6N and 9; Supplemental Figure 13). The formation of ternary proteins brings HAT modifiers (Figure 9), and thus high levels of H3K9ac, specifically to drought-responsive genes for increased transcriptional activation (Figure 7A). The intrinsic ABRE-mediated expression of drought-responsive genes can only be activated effectively by ternary proteins: PtrAREB1-2:PtrADA2b-3:PtrGCN5-1 (Figure 7A). In addition, only the ternary complex containing PtrGCN5-1 can boost the enrichment of H3K9ac at the promoter of drought-responsive genes (Figure 7B), creating "open" chromatin states (Berger, 2007) for elevated gene expression. Such chromatin states allow the enhanced recruitment of RNA Pol II at *PtrNAC* gene promoters for transcription. This enhanced recruitment also needs the ternary complex (Figure 9).

TFs that recruit members of SAGA-like protein complexes for transcriptional regulation in plant development have been reported previously (Mao et al., 2006; Weiste and Dröge-Laser, 2014; Zhou et al., 2017). The SAGA complex is a highly conserved transcriptional coactivator in plants and other organisms (Brownell et al., 1996; Grant et al., 1997; Koutelou et al., 2010; Bonnet et al., 2014; Zhou et al., 2017). The Arabidopsis TF bZIP11 interacts with ADA2b, activating auxin-induced transcription (Weiste and Dröge-Laser, 2014). A recent study showed that the rice homeodomain protein WOX11 recruits the ADA2-GCN5 HAT module to regulate crown root cell proliferation (Zhou et al., 2017). We uncovered a coordinated regulation of histone modifications and regulatory TFs requiring a combinatorial function of the regulatory TF and two SAGA members for the transcriptional activation of drought-responsive genes. This combinatorial function is supported by in planta evidence. RNAi or CRISPR-mediated mutation of any one of the ternary members reduces the drought-activated states of the drought-responsive *PtrNAC* genes and the H3K9ac and RNA Pol II enrichment levels at the promoters of these *NAC* genes (Figures 8A to 8I). As a result, the drought survival rates of these RNAi transgenics and CRISPR mutants were reduced drastically from ~76% (the wild type, with very mild drought treatment) to ~19 to 30% (Figures 8J and 8K).

Under drought conditions, plants alter their physiology to reduce growth and enhance drought tolerance for adaptation (Skirycz and Inzé, 2010). Such adaptation includes adjustments of stomatal closure (Hu et al., 2006), root architecture (Lee et al., 2017), and hydraulic conductance (Hochberg et al., 2017). Hydraulic conductivity in xylem is related to xylem water potential (Choat et al., 2012) and vessel diameter (Tyree and Sperry, 1989; Fisher et al., 2007). A decrease in water potential reduces hydraulic conductivity (Tyree and Sperry, 1989; Choat et al., 2012) and leads to failure in upward water transport through the xylem, known as xylem cavitation or embolism (Tyree and Sperry, 1989). Plants with smaller vessel diameter can endure lower water potential to prevent xylem cavitation (Fisher et al., 2007). All the *OE-PtrNAC* transgenics produced here have higher stem water potential (Figure 3D), smaller vessel lumen area (Figures 4A, 4B, and 4E), and more vessel cells (Figures 4A and 4C) than wild-type controls. These cellular phenotypes indicate that the coordinated regulation of histone modifications and TFs may link to signaling pathways leading to reprogrammed cell differentiation to minimize xylem cavitation for survival. Thus, our work uncovers a potential molecular mechanism involved in regulating plant hydraulic conductance in response to drought stress.

For the coordinated regulatory system discovered in this study, we focused only on a set of key factors (*AREB1*, *ADA2b*, and *GCN5*). In the genome of *P. trichocarpa*, there are four *AREB1*, three *ADA2b*, and two *GCN5* homologs (Supplemental Data Set 6). We also discovered that the regulation activates many other TF genes and genes with promoters containing ABRE motifs (at least 76 key TF genes). We do not know the roles of these other genes. They also may be involved directly in drought response and tolerance, or in other traits such as cellular activities, that may contribute additionally to the development of drought tolerance.

In addition to the unique cellular development, we also observed retarded growth (Supplemental Figures 16A and 16B) in transgenics overexpressing *PtrAREB1-2*. However, these transgenics are completely drought tolerant after a continuous dehydration of 12 d (100% survival rate; Supplemental Figures 16A and 16C). Slight growth reduction also occurred in transgenic *OE-PtrNAC006* plants, which too exhibited a high survival rate (76%; Figures 3A and 3C). After the 12-d drought (water-withholding) experiments, the potting soil in which these two types of transgenics were grown remained sufficiently moist, whereas the soil of wild-type control plants was dried out. Therefore, these transgenics have reprogrammed their growth to allow reduced transpiration and increased water use efficiency to maintain a level of stem hydraulic conductivity conducive to growth. These drought-tolerant plants also are highly drought resilient and grow normally after drought stress, with a growth rate similar to that of normal wild-type *P. trichocarpa*. Such transgenics should grow well on marginal land not suitable for conventional agriculture. Field testing of these transgenics/mutants will reveal additional regulation, enabling further strategic reengineering to maximize growth and other beneficial traits while minimizing the negative effects of drought stress. The approaches reported here need to be explored in other tree species. A sustainable and abundant woody feedstock continues to be an essential renewable resource worldwide.

METHODS

Plant Materials and Growth Conditions

Populus trichocarpa genotype Nisqually-1 was used for all experiments. Wild-type and transgenic plants were grown in a walk-in growth chamber

(21 to 25°C, 16-h-light/8-h-dark cycle with supplemental light of ~300 μE $m^{-2} s^{-1}$, three-band linear fluorescent lamp T5 28W 6400K, and 60 to 80% humidity) as described previously (Song et al., 2006). Soil was composed of peat moss and Metro-Mix200 in a 2:1 ratio at identical dry weight per pot and was watered daily to maintain a water content of ~0.75 g of water per g of dry soil. In ChIP-seq and RNA-seq experiments, 3-month-old clonally propagated wild-type *P. trichocarpa* plants in 15-cm pots (one plant per pot) having the same size and vigor were used for drought treatments (soil water depletion), following established procedures (Arango-Velez et al., 2011). *P. trichocarpa* plants were divided into three groups: (1) control, (2) 5-d drought treatment (no watering), and (3) 7-d drought treatment (no watering). All plants were equally well watered prior to drought treatment. Watering of group 3 plants ceased first, for 7 d (D7). Two days later, watering of group 2 plants ceased for 5 d (D5). Watering of group 1 control plants was continued on a daily basis (ND) for the entire period of the drought treatments for groups 3 and 2. In this way, all plants were harvested on the same day (day 7) and at the same time (~10 AM) for SDX tissue collection (Supplemental Figure 1C). SDX tissue for ChIP-seq was collected from debarked stem, treated with formaldehyde to stabilize protein-DNA interactions, and then frozen in liquid nitrogen and stored at −80°C until use, as described previously (Lin et al., 2013; Li et al., 2014). SDX tissue for RNA-seq was collected directly into liquid nitrogen and stored in liquid nitrogen (Li et al., 2012; Lin et al., 2013).

ChIP Assays in *P. trichocarpa* Differentiating Xylem

ChIP was performed on the SDX of 3-month-old *P. trichocarpa* plants following an established protocol (Lin et al., 2013; Li et al., 2014). Briefly, ~5 g of SDX tissue was cross-linked in 1% (w/v) formaldehyde and used to isolate nuclei and chromatin. The chromatin was sheared into 200- to 1000-bp fragments, subjected to immunoprecipitation using 5 μg of anti-H3K9ac (Abcam, ab10812) or anti-RNA Pol II (ab817) antibodies, and collected with protein G magnetic beads (Invitrogen). Precipitated chromatin was de-cross-linked to release the ChIP-DNA, which was purified and quantified (Qubit Fluorometer) for ChIP-qPCR detection or ChIP-seq library construction. Primers for ChIP-qPCR are listed in Supplemental Table 3. For ChIP-seq, 12 libraries (2 DNA samples [ChIP-DNA and input DNA] × 2 biological replicates [independent pools of *P. trichocarpa* SDX tissue] × 3 [one control, ND + two treatments, D5 and D7]) were prepared using a library preparation kit (New England Biolabs) according to the manufacturer's instructions and sequenced using an Illumina Genome Analyzer.

ChIP-seq Data Analysis

Reads with an average length of 100 bp were obtained. After removing the library index sequences from each read, the remaining sequence reads were mapped to the *P. trichocarpa* genome v.3.0 using Bowtie2 (version 2.1.0; parameters: bowtie2 -p 8 -x P.trichocarpa.index -1 read1.fq.gz -2 read2.fq.gz -S mapping.sam) (Langmead and Salzberg, 2012). The alignments with no more than three mismatches were retained for further analysis. The quality of the raw data was evaluated with FastQC (http://www.bioinformatics.babraham.ac.uk/projects/fastqc/), and low-quality reads were filtered by Sickle (https://github.com/najoshi/sickle/). Peak calling to identify the range and pattern of H3K9ac and the detection of differential modifications between the drought-treated and well-watered samples were performed using diffReps (Shen et al., 2013) with default parameters (diffReps.pl–meth nb–pval 0.0001–treatment D5/D7_IP.bed–control ND_IP.bed–btr D5/D7_input.bed–bco ND_input.bed–report diffReps_peaks–chrlen PtrChrLen.txt–nproc 7). The replicate reproducibility was evaluated by the negative binomial test. The Benjamini-Hochberg adjusted P value (adjusted $P < 0.05$) in diffReps analysis was used to select differential H3K9ac peaks between the drought-treated and well-watered samples.

Total RNA Extraction

Total RNA from SDX or SDX protoplasts of *P. trichocarpa* plants was extracted using a Qiagen RNeasy Plant Mini Kit (Qiagen) as described previously (Lin et al., 2013, 2014). RNA quality was examined using a Bioanalyzer 2100 (Agilent). The RNA was used for RNA-seq, gene cloning, and RT-qPCR.

RNA-seq Analysis

RNA-seq was performed for SDX tissues isolated from the same *P. trichocarpa* plants used for ChIP-seq. Total RNA (1 μg) of each sample was used for library construction using an Illumina TruSeq RNA sample preparation kit. The quality and concentration of libraries were examined using a Bioanalyzer 2100 (Agilent). A total of 12 libraries (4 biological replicates [independent pools of *P. trichocarpa* SDX tissue] × 3 [1 control, ND + 2 treatments, D5 and D7]) were sequenced using an Illumina Genome Analyzer, and 100-bp average read lengths were obtained. After removing the library index sequences from each read, the remaining RNA-seq reads were mapped to the *P. trichocarpa* genome v.3.0 using TopHat (Kim et al., 2013) with default parameters (tophat–read-mismatches 2 -p 8 P.trichocarpa.index sample_1.fq.gz sample_reads_2.fq.gz). The frequency of raw counts was determined by BEDTools (Quinlan and Hall, 2010) for all annotated genes. DEGs between the drought-treated and well-watered samples were identified using edgeR (Robinson et al., 2010) based on raw counts of mapped RNA-seq reads to annotated genes and following an established analysis pipeline (Lin et al., 2013) with FDR < 0.05. GO analyses were conducted using the online tool PANTHER (http://www.pantherdb.org/geneListAnalysis.do; Mi et al., 2013) by Fisher's exact test with FDR multiple test correction (FDR < 0.05).

Integrative Analysis of ChIP-seq and RNA-seq

BETA (Wang et al., 2013) was used to integrate ChIP-seq and RNA-seq data for *P. trichocarpa* with minor modifications. BETA uses a Rank Product algorithm to screen for target genes of histone modification based on both the proximity of the modification to the TSS of the gene and the differential expression level of the gene. Drought-responsive DEGs with differential H3K9ac peaks (FDR < 0.05) within ±2 kb of the TSS of the drought-responsive DEGs were identified by the modified BETA (BETA minus -p diffReps_peaks -r Ptr.refgene -d 2000 -n diffReps_gene.results). Gene expression information and the differential H3K9ac peaks for the identified drought-responsive DEGs were integrated to reveal correlations between H3K9ac (hUP or hDN) and gene expression (gUP or gDN) using R scripts (Wickham, 2009). The abundance of consensus motifs in the 2-kb promoters of the identified drought-responsive DEGs with differential H3K9ac was assessed using AME (McLeay and Bailey, 2010) with Fisher's exact test.

Phylogenetic Analysis

A phylogenetic tree was reconstructed using MEGA 5 with the neighbor-joining method and 1000 bootstrap replicates. Alignments used to produce phylogenies are provided as Supplemental Data Sets 7 and 8.

RT-qPCR

RT-qPCR was performed as described previously (Li et al., 2012) to detect gene expression in SDX tissue or SDX protoplasts of *P. trichocarpa* plants. cDNAs were synthesized by reverse transcription with SuperScript III Reverse Transcriptase (Invitrogen) according to the manufacturer's protocol. RT-qPCR was performed using FastStart Universal SYBR Green Master (Roche) on an Agilent Mx3000P Real-Time PCR System. PCR

amplification was in the logarithmic phase for each DNA molecule being analyzed.

Generation and Analysis of *P. trichocarpa* Transgenic and Mutant Plants

Coding regions of *PtrNAC006*, *PtrNAC007*, *PtrNAC120*, and *PtrAREB1-2* were amplified from *P. trichocarpa* plants and, after sequence confirmation, inserted into the pBI121 vector under the control of the CaMV 35S promoter to generate overexpression constructs. RNAi constructs were designed for the downregulation of *PtrAREB1-2* and *PtrGCN5-1* genes. Specific sequences of the two RNAi target genes were amplified and assembled with a 600-bp GUS linker sequence to form RNAi transgene sequences and then cloned into pCR2.1 vector. After sequencing, the assembled RNAi transgene fragments were subcloned into the pBI121 vector to obtain RNAi constructs. Knockout mutants of *PtrADA2b-3* were generated using the CRISPR-Cas9 system (Ueta et al., 2017). The single guide RNA (sgRNA) sequence (Supplemental Table 3) targeting *PtrADA2b-3* was selected using CRISPR-P 2.0 (http://crispr.hzau.edu.cn/cgi-bin/CRISPR2/CRISPR). sgRNA target sequences with sticky ends created by *Bsa*I were synthesized and inserted into pEgP237-2A-GFP vector digested with *Bsa*I (Ueta et al., 2017). All plasmids were introduced into *Agrobacterium tumefaciens* strain C58 for *P. trichocarpa* transformation as described previously (Song et al., 2006).

The expression of *PtrNAC* genes, *PtrAREB1-2*, and *PtrGCN5-1* in transgenic plants was determined by RT-qPCR as described above. For detection of the *PtrADA2b-3* mutation, PCR amplification was performed using primers flanking the sgRNA target sequence. The PCR products (300–500 bp) were inserted into pMD18-T vector (Takara, 6011), and 20 colonies were selected for sequencing. Primers for vector construction, mutation detection, and RT-qPCR are listed in Supplemental Table 3. The transgenic *P. trichocarpa* lines with the highest transgene transcript levels for *PtrNAC* genes and *PtrAREB1-2*, and with two distinct levels (highest and intermediate suppression) of target gene knockdown for *PtrAREB1-2* and *PtrGCN5-1*, were selected and maintained in a walk-in growth chamber for further analysis. Transgenic, mutant, and wild-type plants were grown in 15-cm pots (one plant per pot) with the same amount of soil as described above. Drought treatment was applied to 3-month-old plants of ~50 cm height by withholding water. To allow drought-treated plants to recover, plants overexpressing *PtrNAC* genes and *PtrAREB1-2* as well as wild-type control plants were rewatered after 12 d of drought treatment, and RNAi-*PtrAREB1-2*, RNAi-*PtrGCN5-1*, KO-*PtrADA2b-3*, and wild-type plants were rewatered after 10 d. Survival rates were calculated based on the plants that survived after rewatering for 3 d. At least 12 transgenic plants for each gene construct and 12 wild-type plants were tested in each drought treatment experiment. Water potential was measured under well-watered conditions and with drought treatment for 5 d. Six transgenic plants for each gene construct and six wild-type plants were used in each test. A SAPS II Water Potential System (SEC) was used for the measurement of stem water potential according to the manufacturer's instructions. Statistical analyses were performed based on data from three independent experiments.

Histochemical and Histological Analyses

Stem segments were harvested from the 10th internode of *OE-PtrNAC006*, *OE-PtrNAC007*, and *OE-PtrNAC120* transgenic and wild-type plants. Each segment was cut into 2-mm fragments and fixed with 4% (w/v) paraformaldehyde in 1× phosphate-buffered saline buffer at 4°C for 12 h. Fixed materials were washed with 1× phosphate-buffered saline, dehydrated in a graded ethanol series, incubated sequentially in ethanol:xylene 75:25, 50:50, 25:75, and 0:100% (v/v), and embedded in paraffin (Sigma-Aldrich). The embedded fragments were sectioned to a thickness of 16 μm using a rotary microtome (Leica RM2245) and deparaffinized using xylene. Sections were stained with safranin O and fast green and observed with a microscope (Leica DM6B). The parameters of individual vessels were measured using LAS V4.8 and LAS X V2.0 software (Leica). More than 30 measurements for each transgenic line and the wild type with three independent replicates were performed for statistical analysis.

Scanning Electron Micrograph Analysis

Fresh stem segments of the 10th internode of *OE-PtrNAC006*, *OE-PtrNAC007*, and *OE-PtrNAC120* transgenic and wild-type plants were harvested and coated with gold at 10 mA for 60 s. The samples were transferred to a scanning electron microscopy chamber and imaged under high vacuum at 15 kV using a Nanotech JCM-5000.

Gene Expression Analysis in SDX Protoplasts

The full coding sequences of *PtrAREB1-2*, *PtrGCN5-1*, and *PtrADA2b-3* were cloned into pENTR/D-TOPO vector (Invitrogen) and then recombined into the pUC19-$35S_{pro}$-*RfA*-$35S_{pro}$-*sGFP* (Li et al., 2012) destination vector, generating pUC19-$35S_{pro}$-*PtrAREB1-2*-$35S_{pro}$-*sGFP*, pUC19-$35S_{pro}$-*PtrGCN5-1*-$35S_{pro}$-*sGFP*, and pUC19-$35S_{pro}$-*PtrADA2b-3*-$35S_{pro}$-*sGFP*, respectively. *PtrAREB1-2* without stop codon was inserted into the pUC19-$35S_{pro}$-*sGFP* (Li et al., 2012) vector, generating pUC19-$35S_{pro}$-*PtrAREB1-2*-*sGFP*. *PtrADA2b-3* was then cloned into pUC19-$35S_{pro}$-*PtrAREB1-2*-*sGFP*, giving pUC19-$35S_{pro}$-*PtrAREB1-2-PtrADA2b-3*. The constructs pUC19-$35S_{pro}$-*PtrAREB1-2-PtrGCN5-1* and pUC19-$35S_{pro}$-*PtrADA2b-3-PtrGCN5-1* were generated in a similar way. *PtrAREB1-2* without stop codon was cloned into pUC19-$35S_{pro}$-*PtrADA2b-3-PtrGCN5-1*, generating pUC19-$35S_{pro}$-*PtrAREB1-2-PtrADA2b-3-PtrGCN5-1*. The plasmids were prepared using a CsCl gradient and transfected into SDX protoplasts as described previously (Lin et al., 2013, 2014). After culturing for 12 h, protoplasts were collected for RNA extraction and RT-qPCR analysis as described above. Three biological replicates for each transfection and three technical repeats for each biological replicate were performed. Primers for construct generation and RT-qPCR are listed in Supplemental Table 3.

ChIP Assays in SDX Protoplasts

Plasmids as described above were prepared using a CsCl gradient and transfected into SDX protoplasts as described previously (Lin et al., 2013, 2014) for ChIP assays. Approximately 6 mg of plasmid DNA and ~1×10^7 SDX protoplasts were used for each transfection. ChIP assays in SDX protoplasts were performed as described previously (Lin et al., 2013; Li et al., 2014) with a few modifications. In brief, protoplasts were collected for cross-linking with 1% (w/v) formaldehyde in WI buffer (0.2 M MES, pH 5.7, 0.8 M mannitol, and 2 M KCl) for 10 min at room temperature. The cross-linked protoplasts were collected for chromatin extraction and sonication using a Bioruptor (Diagenode) for three rounds of five cycles. Sonicated chromatin was immunoprecipitated using 5 μg of anti-GFP (Abcam, ab290), anti-H3K9ac (ab10812), or anti-RNA Pol II (ab817) antibodies. Purified ChIP-DNAs were analyzed by ChIP-qPCR as described previously (Li et al., 2014). Three biological replicates for each transfection and three technical repeats for each biological replicate were performed. Primers for ChIP-qPCR are listed in Supplemental Table 3.

Pull-Down Assays

For pull-down assays, pETDuet-1 vector (Novagen) was used to coexpress two target genes driven by two independent T7 promoters. The coding sequences of *PtrAREB1-2* and *PtrADA2b-3* were cloned into pETDuet-1 vector at the first multiple cloning site with a 6×His tag and the second multiple cloning site with an S tag, to generate a construct harboring

PtrAREB1-2:*6×His-tag* and *PtrADA2b-3*:*S-tag*. In the same way, constructs harboring *PtrGCN5-1*:*6×His-tag* and *PtrADA2b-3*:*S-tag*, *PtrGCN5-1*:*6×His-tag* and *PtrAREB1-2*:*S-tag*, *PtrAREB1-2*:*6×His-tag* and *GFP*:*S-tag*, and *PtrGCN5-1*:*6×His-tag* and *GFP*:*S-tag* were assembled, and *GFP* was used as a negative control. Primers for construct generation are listed in Supplemental Table 3. The constructs were transferred into *Escherichia coli* BL21 to produce fusion proteins. Briefly, bacteria were cultured in Luria-Bertani medium at 37°C until OD_{600} reached 0.4 to 0.6 and then continuously cultured at 25°C for 6 h after adding 0.5 mM IPTG. Cells were collected and lysed in lysis buffer (50 mM Tris-HCl, pH 8.0, 500 mM NaCl, 10 mM imidazole, 10% (v/v) glycerol, 0.1% (v/v) Tween-20, and 2 mM PMSF) by sonication. The supernatants from the cell lysates were collected and incubated with HisPur Ni-NTA Resin (Thermo Scientific) for 2 h at 4°C. After washing the beads eight times with wash buffer (50 mM Tris-HCl, pH 8.0, 500 mM NaCl, 15 mM imidazole, 10% (v/v) glycerol, and 1.5 mM β-mercaptoethanol), the bound proteins were eluted with elution buffer (50 mM Tris-HCl, pH 8.0, 500 mM imidazole, and 1.5 mM β-mercaptoethanol) and collected using Centrifugal Filter Devices (Millipore). His- and S-tagged proteins were detected using anti-His (Abcam, ab1187) and anti-S (ab184223) antibodies, respectively.

Immunoblotting

Proteins were separated by 10% (w/v) SDS-PAGE and subsequently blotted onto a PVDF membrane (Thermo Scientific). The membrane was blocked using nonfat dry milk and then probed with the indicated antibodies (anti-His antibody, Abcam, ab1187; anti-S antibody, ab184223). Signals were detected using SuperSignal West Pico Chemiluminescent Substrate (Thermo Scientific) and x-ray film (Sigma-Aldrich).

EMSA

The full-length coding sequence of *PtrAREB1-2* was cloned into pETDuet-1 vector (Novagen) with a 6×His tag at its N terminus using *Bam*HI/*Hind*III restriction enzymes. The construct was transferred into *E. coli* BL21 for recombinant protein production. Recombinant protein was purified using HisPur Ni-NTA Resin (Thermo Scientific) as described for pull-down assays and collected in concentration buffer (50 mM Tris-HCl, pH 8.0, and 100 mM NaCl) using Centrifugal Filter Devices (Millipore). An empty pETDuet-1 vector was used as a negative control. DNA fragments from *PtrNAC006*, *PtrNAC007*, and *PtrNAC120* promoters, harboring the ABRE motif, were biotin labeled at the 3′ end using a Biotin 3′ End DNA labeling kit (Thermo Scientific). All ABRE motifs in the promoter fragments also were mutated by changing the first T to A for the synthesis of mutated probes. Primers for construct generation and probe preparation are listed in Supplemental Table 3.

EMSA was performed using a Lightshift Chemiluminescent EMSA kit (Thermo Scientific) according to the manufacturer's instructions. Briefly, biotin-labeled probes were mixed with 100 ng of purified proteins for 20 min in binding buffer (10 mM Tris-HCl, pH 7.5, 50 mM KCl, 1 mM DTT, 2.5% (v/v) glycerol, 5 mM $MgCl_2$, 0.05% (v/v) Nonidet P-40, and 100 ng/μL poly[dI-dC]) at room temperature. Wild-type or mutated unlabeled probes were used as competitors in competition analyses in 50-, 100-, and 150-fold molar excess relative to the labeled probes. Protein-DNA mixtures were separated on a 6.5% (w/v) native PAGE gel and transferred to a nylon membrane (Thermo Scientific). Signals were detected by chemiluminescence.

BiFC Assays

The coding sequences of *PtrADA2b-3*, *PtrAREB1-2*, and *PtrGCN5-1* were cloned into pENTR/D-TOPO vector (Invitrogen), and sequence-confirmed PCR fragments were recombined into a BiFC destination vector. Primers for BiFC vector construction are listed in Supplemental Table 3. Each pair of vectors (*ADA2b-3*:YFP^N/*GCN5-1*:YFP^C, *ADA2b-3*:YFP^N/*AREB1-2*:YFP^C, and *AREB1-2*:YFP^N/*GCN5-1*:YFP^C) was cotransfected into SDX protoplasts with *H2A-1*:*mCherry* following an established protocol (Lin et al., 2014). Cotransfection of each protein of interest with empty plasmid was performed as a negative control. An unrelated nuclear protein, PtrMYB021, was used as another negative control. *ADA2b-3*:YFP^N/*MYB021*:YFP^C, *MYB021*:YFP^N/*AREB1-2*:YFP^C, and *MYB021*:YFP^N/*GCN5-1*:YFP^C were cotransfected independently with *H2A-1*:*mCherry* into SDX protoplasts. After incubation for 12 h, SDX protoplasts were collected and examined with a confocal laser scanning microscope (Zeiss LSM 700). Therefore, one entire run of BiFC included nine experiments for three pairs of the tested dimers and two sets of negative controls. The entire run was repeated three times using three different batches of SDX protoplasts (i.e., three biological replicates). The SDX protoplast system typically has a transformation rate of 30 to 40% (Lin et al., 2014). In each of the nine experiments (in one biological replicate), 50 to 60 individual protoplast cells were examined and at least 12 individual protoplast cells with the specific fluorescent signals from cotransfected proteins could normally be identified. One image was selected, such as shown in Figure 6F, from these ~12 cells from each experiment. The images of a set of nine experiments for one biological replicate are shown in Figures 6F to 6N. Images from the other two biological replicates are shown in Supplemental Figures 13A to 13R.

Statistical Analysis

Student's *t* test was performed using SPSS software (v.19.0) to determine significance, which was defined as *, $P < 0.05$ and **, $P < 0.01$. Detailed results of statistical analyses are available as Supplemental File 1.

Accession Numbers

The ChIP-seq and RNA-seq data for this work have been deposited in the National Center for Biotechnology Information Gene Expression Omnibus database under accession number GSE81048. Sequence data from this article can be found in *Populus trichocarpa* v3.0 (Poplar) of Phytozome 12 under the following accession numbers: *PtrNAC005* (Potri.005G069500), *PtrNAC006* (Potri.002G081000), *PtrNAC118* (Potri.011G123300), *PtrNAC007* (Potri.007G099400), *PtrNAC120* (Potri.001G404100), *PtrAREB1-2* (Potri.002G125400), *PtrAREB1-3* (Potri.009G101200), *PtrAREB1-4* (Potri.014G028200), *PtrADA2b-3* (Potri.004G135400), *PtrGCN5-1* (Potri.002G045900), *PtrMYB021* (Potri.009G053900), *PtrNAC047* (Potri.013G054000), *PtrNAC071* (Potri.019G099900), *PtrNAC083* (Potri.017G063300), *PtrNAC091* (Potri.019G099800), and *PtrNAC100* (Potri.017G086200).

Supplemental Data

Supplemental Figure 1. Drought Treatment of *P. trichocarpa* Followed by Genome-Wide Investigation of H3K9ac and Transcriptomic Analysis in SDX Tissues.

Supplemental Figure 2. Genome-Wide Analysis of H3K9ac in SDX Tissues of *P. trichocarpa* under Well-Watered and Drought Conditions.

Supplemental Figure 3. RNA-seq Volcano Plots for D5/ND and D7/ND.

Supplemental Figure 4. Main Enriched GO Categories among Upregulated or Downregulated Genes Identified from D5 and D7 Treatments.

Supplemental Figure 5. Integration of ChIP-seq and RNA-seq Data to Identify Drought Stress-Responsive Genes Associated with H3K9ac at Promoter and/or Gene Body Regions.

Supplemental Figure 6. Phylogenetic Tree of *NAC* Genes in *P. trichocarpa* and Arabidopsis.

Supplemental Figure 7. Phenotypes and Transgene Expression Levels in the Stem Developing Xylem of Four Independent *PtrNAC006* Transgenic Lines.

Supplemental Figure 8. Transcript Levels of *PtrNAC006*, *PtrNAC007*, and *PtrNAC120* and Growth Data for Wild-Type and Transgenic Plants under Well-Watered and Drought Conditions.

Supplemental Figure 9. Scanning Electron Micrographs of Wild-Type, *OE-PtrNAC007*, and *OE-PtrNAC120* Transgenic Plants.

Supplemental Figure 10. Phylogenetic Tree of *AREB1* Genes in *P. trichocarpa* and Arabidopsis.

Supplemental Figure 11. Relative Transcript Levels of *PtrNAC006*, *PtrNAC007*, and *PtrNAC120* in SDX Protoplasts Overexpressing *PtrAREB1-2* or *GFP* in the Absence of External ABA.

Supplemental Figure 12. Cloning of the *PtrADA2b* Gene and Schematic Diagram of Its Splice Variants.

Supplemental Figure 13. Biological Replicates of the BiFC Assay Data.

Supplemental Figure 14. PtrAREB1-2:PtrADA2b-3:PtrGCN5-1 Induces Activation of the Three *NAC* Genes in the Absence of External ABA.

Supplemental Figure 15. Identification RNAi-*PtrAREB1-2*, RNAi-*PtrGCN5-1*, and Knockout-*PtrADA2b-3* Plants.

Supplemental Figure 16. Overexpressing the *PtrAREB1-2* Gene Improves Drought Stress Tolerance of *P. trichocarpa*.

Supplemental Table 1. ChIP-seq for Identification of Differential H3K9ac Peaks under Drought Stress.

Supplemental Table 2. RNA-seq for Identification of DEGs under Drought Stress.

Supplemental Table 3. Primer List.

Supplemental Data Set 1. Integrative Analysis of ChIP-seq and RNA-seq Data for D5/ND.

Supplemental Data Set 2. Integrative Analysis of ChIP-seq and RNA-seq Data for D7/ND.

Supplemental Data Set 3. GO Enrichment Analysis of the hUP-gUP and hDN-gDN Set of Genes in D5 and D7.

Supplemental Data Set 4. ABRE-Containing TF Genes for D5/ND.

Supplemental Data Set 5. ABRE-Containing TF Genes for D7/ND.

Supplemental Data Set 6. RNA-seq Data of *PtrGCN5*, *PtrADA2b*, *PtrAREB1*, *PtrNACs*, and *PtrGBF3* Genes.

Supplemental Data Set 7. Alignments Used to Produce Phylogenies of NACs.

Supplemental Data Set 8. Alignments Used to Produce Phylogenies of AREB1s.

Supplemental File 1. Statistical Analysis.

ACKNOWLEDGMENTS

We thank Keishi Osakabe for CRISPR/Cas9 constructs. This work was supported by the National Key Research and Development Program of China (2016YFD0600106), the National Natural Science Foundation of China (31522014, 31570663, and 31430093), the Fundamental Research Funds for the Central Universities (2572018CL02), and the Innovation Project of State Key Laboratory of Tree Genetics and Breeding (Northeast Forestry University) (to W.L.). We are also grateful for financial support from the '1000-Talents Plan' for young researchers from China and the Longjiang Young Scholar Program of Heilongjiang Provincial Government (to W.L.), the U.S. Office of Science (Biological and Environmental Research), Department of Energy (DE-SC000691 to V.L.C.), the Taiwan Ministry of Science and Technology MOST (106-2311-B-002-001-MY2 and 107-2636-B-002-003 to Y.-C.J.L.), and the 111 Project (B16010).

AUTHOR CONTRIBUTIONS

W.L., V.L.C., Y.-C.J.L., and J.P.W. conceived the research and designed the experiments. S.L., Y.-C.J.L., P.W., B.Z., M.L., X.L., Z.W., X.D., J.Y., C.Z., and B.L. performed the experiments. S.C., R.S., and S.T.-A. contributed new analytic/computational tools. W.L., V.L.C., Y.-C.J.L., and S.L. analyzed the data and wrote the manuscript with input from all coauthors.

Received June 7, 2018; revised October 29, 2018; accepted November 24, 2018; published December 11, 2018.

REFERENCES

Arango-Velez, A., Zwiazek, J.J., Thomas, B.R., and Tyree, M.T. (2011). Stomatal factors and vulnerability of stem xylem to cavitation in poplars. Physiol. Plant. **143:** 154–165.

Ascenzi, R., and Gantt, J.S. (1999). Molecular genetic analysis of the drought-inducible linker histone variant in Arabidopsis thaliana. Plant Mol. Biol. **41:** 159–169.

Aubert, Y., Vile, D., Pervent, M., Aldon, D., Ranty, B., Simonneau, T., Vavasseur, A., and Galaud, J.P. (2010). RD20, a stress-inducible caleosin, participates in stomatal control, transpiration and drought tolerance in *Arabidopsis thaliana*. Plant Cell Physiol. **51:** 1975–1987.

Balasubramanian, R., Pray-Grant, M.G., Selleck, W., Grant, P.A., and Tan, S. (2002). Role of the Ada2 and Ada3 transcriptional coactivators in histone acetylation. J. Biol. Chem. **277:** 7989–7995.

Barber, V.A., Juday, G.P., and Finney, B.P. (2000). Reduced growth of Alaskan white spruce in the twentieth century from temperature-induced drought stress. Nature **405:** 668–673.

Barbosa, E.G.G., et al. (2013). Overexpression of the ABA-dependent AREB1 transcription factor from *Arabidopsis thaliana* improves soybean tolerance to water deficit. Plant Mol. Biol. Rep. **31:** 719–730.

Berger, S.L. (2007). The complex language of chromatin regulation during transcription. Nature **447:** 407–412.

Berta, M., Giovannelli, A., Sebastiani, F., Camussi, A., and Racchi, M.L. (2010). Transcriptome changes in the cambial region of poplar (*Populus alba* L.) in response to water deficit. Plant Biol. (Stuttg.) **12:** 341–354.

Bogeat-Triboulot, M.B., et al. (2007). Gradual soil water depletion results in reversible changes of gene expression, protein profiles, ecophysiology, and growth performance in *Populus euphratica*, a poplar growing in arid regions. Plant Physiol. **143:** 876–892.

Bonnet, J., Wang, C.Y., Baptista, T., Vincent, S.D., Hsiao, W.C., Stierle, M., Kao, C.F., Tora, L., and Devys, D. (2014). The SAGA coactivator complex acts on the whole transcribed genome and is required for RNA polymerase II transcription. Genes Dev. **28:** 1999–2012.

Brownell, J.E., Zhou, J., Ranalli, T., Kobayashi, R., Edmondson, D. G., Roth, S.Y., and Allis, C.D. (1996). Tetrahymena histone acetyltransferase A: A homolog to yeast Gcn5p linking histone acetylation to gene activation. Cell **84:** 843–851.

Charron, J.B., He, H., Elling, A.A., and Deng, X.W. (2009). Dynamic landscapes of four histone modifications during deetiolation in *Arabidopsis*. Plant Cell **21:** 3732–3748.

Choat, B., et al. (2012). Global convergence in the vulnerability of forests to drought. Nature **491:** 752–755.

Evert, R.F. (2006). Esau's Plant Anatomy: Meristems, Cells, and Tissues of the Plant Body: Their Structure, Function, and Development, . (Hoboken, NJ: John Wiley & Sons).

Fisher, J.B., Goldstein, G., Jones, T.J., and Cordell, S. (2007). Wood vessel diameter is related to elevation and genotype in the Hawaiian tree *Metrosideros polymorpha* (Myrtaceae). Am. J. Bot. **94:** 709–715.

Fujita, M., Fujita, Y., Maruyama, K., Seki, M., Hiratsu, K., Ohme-Takagi, M., Tran, L.S., Yamaguchi-Shinozaki, K., and Shinozaki, K. (2004). A dehydration-induced NAC protein, RD26, is involved in a novel ABA-dependent stress-signaling pathway. Plant J. **39:** 863–876.

Fujita, Y., Fujita, M., Satoh, R., Maruyama, K., Parvez, M.M., Seki, M., Hiratsu, K., Ohme-Takagi, M., Shinozaki, K., and Yamaguchi-Shinozaki, K. (2005). AREB1 is a transcription activator of novel ABRE-dependent ABA signaling that enhances drought stress tolerance in *Arabidopsis*. Plant Cell **17:** 3470–3488.

Fujita, Y., Fujita, M., Shinozaki, K., and Yamaguchi-Shinozaki, K. (2011). ABA-mediated transcriptional regulation in response to osmotic stress in plants. J. Plant Res. **124:** 509–525.

Furihata, T., Maruyama, K., Fujita, Y., Umezawa, T., Yoshida, R., Shinozaki, K., and Yamaguchi-Shinozaki, K. (2006). Abscisic acid-dependent multisite phosphorylation regulates the activity of a transcription activator AREB1. Proc. Natl. Acad. Sci. USA **103:** 1988–1993.

Grant, P.A., Duggan, L., Côté, J., Roberts, S.M., Brownell, J.E., Candau, R., Ohba, R., Owen-Hughes, T., Allis, C.D., Winston, F., Berger, S.L., and Workman, J.L. (1997). Yeast Gcn5 functions in two multisubunit complexes to acetylate nucleosomal histones: characterization of an Ada complex and the SAGA (Spt/Ada) complex. Genes Dev. **11:** 1640–1650.

Hark, A.T., Vlachonasios, K.E., Pavangadkar, K.A., Rao, S., Gordon, H., Adamakis, I.D., Kaldis, A., Thomashow, M.F., and Triezenberg, S.J. (2009). Two *Arabidopsis* orthologs of the transcriptional coactivator ADA2 have distinct biological functions. Biochim. Biophys. Acta **1789:** 117–124.

Hickman, R., et al. (2013). A local regulatory network around three NAC transcription factors in stress responses and senescence in *Arabidopsis* leaves. Plant J. **75:** 26–39.

Hochberg, U., Bonel, A.G., David-Schwartz, R., Degu, A., Fait, A., Cochard, H., Peterlunger, E., and Herrera, J.C. (2017). Grapevine acclimation to water deficit: The adjustment of stomatal and hydraulic conductance differs from petiole embolism vulnerability. Planta **245:** 1091–1104.

Hu, H., Dai, M., Yao, J., Xiao, B., Li, X., Zhang, Q., and Xiong, L. (2006). Overexpressing a NAM, ATAF, and CUC (NAC) transcription factor enhances drought resistance and salt tolerance in rice. Proc. Natl. Acad. Sci. USA **103:** 12987–12992.

Hu, R., Qi, G., Kong, Y., Kong, D., Gao, Q., and Zhou, G. (2010). Comprehensive analysis of NAC domain transcription factor gene family in *Populus trichocarpa*. BMC Plant Biol. **10:** 145.

Jaenisch, R., and Bird, A. (2003). Epigenetic regulation of gene expression: How the genome integrates intrinsic and environmental signals. Nat. Genet. **33** (suppl.): 245–254.

Kim, D., Pertea, G., Trapnell, C., Pimentel, H., Kelley, R., and Salzberg, S.L. (2013). TopHat2: Accurate alignment of transcriptomes in the presence of insertions, deletions and gene fusions. Genome Biol. **14:** R36.

Kim, J.M., To, T.K., Ishida, J., Morosawa, T., Kawashima, M., Matsui, A., Toyoda, T., Kimura, H., Shinozaki, K., and Seki, M. (2008). Alterations of lysine modifications on the histone H3 N-tail under drought stress conditions in *Arabidopsis thaliana*. Plant Cell Physiol. **49:** 1580–1588.

Kim, J.M., To, T.K., Ishida, J., Matsui, A., Kimura, H., and Seki, M. (2012). Transition of chromatin status during the process of recovery from drought stress in *Arabidopsis thaliana*. Plant Cell Physiol. **53:** 847–856.

Kornet, N., and Scheres, B. (2009). Members of the GCN5 histone acetyltransferase complex regulate PLETHORA-mediated root stem cell niche maintenance and transit amplifying cell proliferation in Arabidopsis. Plant Cell **21:** 1070–1079.

Koutelou, E., Hirsch, C.L., and Dent, S.Y. (2010). Multiple faces of the SAGA complex. Curr. Opin. Cell Biol. **22:** 374–382.

Kouzarides, T. (2007). Chromatin modifications and their function. Cell **128:** 693–705.

Kurdistani, S.K., Tavazoie, S., and Grunstein, M. (2004). Mapping global histone acetylation patterns to gene expression. Cell **117:** 721–733.

Langmead, B., and Salzberg, S.L. (2012). Fast gapped-read alignment with Bowtie 2. Nat. Methods **9:** 357–359.

Lee, D.Y., Hayes, J.J., Pruss, D., and Wolffe, A.P. (1993). A positive role for histone acetylation in transcription factor access to nucleosomal DNA. Cell **72:** 73–84.

Lee, D.K., Chung, P.J., Jeong, J.S., Jang, G., Bang, S.W., Jung, H., Kim, Y.S., Ha, S.H., Choi, Y.D., and Kim, J.K. (2017). The rice OsNAC6 transcription factor orchestrates multiple molecular mechanisms involving root structural adaptions and nicotianamine biosynthesis for drought tolerance. Plant Biotechnol. J. **15:** 754–764.

Li, Q., Lin, Y.C., Sun, Y.H., Song, J., Chen, H., Zhang, X.H., Sederoff, R.R., and Chiang, V.L. (2012). Splice variant of the SND1 transcription factor is a dominant negative of SND1 members and their regulation in *Populus trichocarpa*. Proc. Natl. Acad. Sci. USA **109:** 14699–14704.

Li, W., Liu, H., Cheng, Z.J., Su, Y.H., Han, H.N., Zhang, Y., and Zhang, X.S. (2011). DNA methylation and histone modifications regulate *de novo* shoot regeneration in *Arabidopsis* by modulating *WUSCHEL* expression and auxin signaling. PLoS Genet. **7:** e1002243.

Li, W., Lin, Y.C., Li, Q., Shi, R., Lin, C.Y., Chen, H., Chuang, L., Qu, G.Z., Sederoff, R.R., and Chiang, V.L. (2014). A robust chromatin immunoprecipitation protocol for studying transcription factor-DNA interactions and histone modifications in wood-forming tissue. Nat. Protoc. **9:** 2180–2193.

Lin, Y.C., et al. (2014). A simple improved-throughput xylem protoplast system for studying wood formation. Nat. Protoc. **9:** 2194–2205.

Lin, Y.C., Li, W., Sun, Y.H., Kumari, S., Wei, H., Li, Q., Tunlaya-Anukit, S., Sederoff, R.R., and Chiang, V.L. (2013). SND1 transcription factor-directed quantitative functional hierarchical genetic regulatory network in wood formation in *Populus trichocarpa*. Plant Cell **25:** 4324–4341.

Mao, Y., Pavangadkar, K.A., Thomashow, M.F., and Triezenberg, S.J. (2006). Physical and functional interactions of *Arabidopsis* ADA2 transcriptional coactivator proteins with the acetyltransferase GCN5 and with the cold-induced transcription factor CBF1. Biochim. Biophys. Acta **1759:** 69–79.

McLeay, R.C., and Bailey, T.L. (2010). Motif Enrichment Analysis: A unified framework and an evaluation on ChIP data. BMC Bioinformatics **11:** 165.

Mi, H., Muruganujan, A., Casagrande, J.T., and Thomas, P.D. (2013). Large-scale gene function analysis with the PANTHER classification system. Nat. Protoc. **8:** 1551–1566.

Monclus, R., Dreyer, E., Villar, M., Delmotte, F.M., Delay, D., Petit, J.M., Barbaroux, C., Le Thiec, D., Bréchet, C., and Brignolas, F. (2006). Impact of drought on productivity and water use efficiency in 29 genotypes of *Populus deltoides* × *Populus nigra*. New Phytol. **169:** 765–777.

Msanne, J., Lin, J., Stone, J.M., and Awada, T. (2011). Characterization of abiotic stress-responsive *Arabidopsis thaliana* RD29A and RD29B genes and evaluation of transgenes. Planta **234:** 97–107.

Nakashima, K., Yamaguchi-Shinozaki, K., and Shinozaki, K. (2014). The transcriptional regulatory network in the drought response and its crosstalk in abiotic stress responses including drought, cold, and heat. Front. Plant Sci. **5:** 170.

Norton, V.G., Imai, B.S., Yau, P., and Bradbury, E.M. (1989). Histone acetylation reduces nucleosome core particle linking number change. Cell **57:** 449–457.

Quinlan, A.R., and Hall, I.M. (2010). BEDTools: A flexible suite of utilities for comparing genomic features. Bioinformatics **26:** 841–842.

Ragauskas, A.J., et al. (2006). The path forward for biofuels and biomaterials. Science **311:** 484–489.

Ramegowda, V., Gill, U.S., Sivalingam, P.N., Gupta, A., Gupta, C., Govind, G., Nataraja, K.N., Pereira, A., Udayakumar, M., Mysore, K.S., and Senthil-Kumar, M. (2017). GBF3 transcription factor imparts drought tolerance in Arabidopsis thaliana. Sci. Rep. **7:** 9148.

Robinson, M.D., McCarthy, D.J., and Smyth, G.K. (2010). edgeR: A Bioconductor package for differential expression analysis of digital gene expression data. Bioinformatics **26:** 139–140.

Roeder, R.G. (1996). The role of general initiation factors in transcription by RNA polymerase II. Trends Biochem. Sci. **21:** 327–335.

Shahbazian, M.D., and Grunstein, M. (2007). Functions of site-specific histone acetylation and deacetylation. Annu. Rev. Biochem. **76:** 75–100.

Shen, L., Shao, N.Y., Liu, X., Maze, I., Feng, J., and Nestler, E.J. (2013). diffReps: Detecting differential chromatin modification sites from ChIP-seq data with biological replicates. PLoS One **8:** e65598.

Skirycz, A., and Inzé, D. (2010). More from less: Plant growth under limited water. Curr. Opin. Biotechnol. **21:** 197–203.

Song, J., Lu, S., Chen, Z.Z., Lourenco, R., and Chiang, V.L. (2006). Genetic transformation of *Populus trichocarpa* genotype Nisqually-1: A functional genomic tool for woody plants. Plant Cell Physiol. **47:** 1582–1589.

Song, L., Huang, S.C., Wise, A., Castanon, R., Nery, J.R., Chen, H., Watanabe, M., Thomas, J., Bar-Joseph, Z., and Ecker, J.R. (2016). A transcription factor hierarchy defines an environmental stress response network. Science **354:** aag1550.

Stockinger, E.J., Mao, Y., Regier, M.K., Triezenberg, S.J., and Thomashow, M.F. (2001). Transcriptional adaptor and histone acetyltransferase proteins in *Arabidopsis* and their interactions with CBF1, a transcriptional activator involved in cold-regulated gene expression. Nucleic Acids Res. **29:** 1524–1533.

Tran, L.S., Nakashima, K., Sakuma, Y., Simpson, S.D., Fujita, Y., Maruyama, K., Fujita, M., Seki, M., Shinozaki, K., and Yamaguchi-Shinozaki, K. (2004). Isolation and functional analysis of *Arabidopsis* stress-inducible NAC transcription factors that bind to a drought-responsive cis-element in the early responsive to dehydration stress 1 promoter. Plant Cell **16:** 2481–2498.

Tyree, M.T., and Sperry, J.S. (1989). Vulnerability of xylem to cavitation and embolism. Annu. Rev. Plant Physiol. Plant Mol. Biol. **1:** 19–36.

Ueta, R., Abe, C., Watanabe, T., Sugano, S.S., Ishihara, R., Ezura, H., Osakabe, Y., and Osakabe, K. (2017). Rapid breeding of parthenocarpic tomato plants using CRISPR/Cas9. Sci. Rep. **7:** 507.

Vlachonasios, K.E., Thomashow, M.F., and Triezenberg, S.J. (2003). Disruption mutations of ADA2b and GCN5 transcriptional adaptor genes dramatically affect *Arabidopsis* growth, development, and gene expression. Plant Cell **15:** 626–638.

Wang, S., Sun, H., Ma, J., Zang, C., Wang, C., Wang, J., Tang, Q., Meyer, C.A., Zhang, Y., and Liu, X.S. (2013). Target analysis by integration of transcriptome and ChIP-seq data with BETA. Nat. Protoc. **8:** 2502–2515.

Weiste, C., and Dröge-Laser, W. (2014). The *Arabidopsis* transcription factor bZIP11 activates auxin-mediated transcription by recruiting the histone acetylation machinery. Nat. Commun. **5:** 3883.

Wickham, H. (2009). ggplot2: Elegant Graphics for Data Analysis. (New York: Springer).

Widiez, T., Symeonidi, A., Luo, C., Lam, E., Lawton, M., and Rensing, S.A. (2014). The chromatin landscape of the moss *Physcomitrella patens* and its dynamics during development and drought stress. Plant J. **79:** 67–81.

Wu, Y., Deng, Z., Lai, J., Zhang, Y., Yang, C., Yin, B., Zhao, Q., Zhang, L., Li, Y., Yang, C., and Xie, Q. (2009). Dual function of *Arabidopsis* ATAF1 in abiotic and biotic stress responses. Cell Res. **19:** 1279–1290.

Yoshida, T., Fujita, Y., Sayama, H., Kidokoro, S., Maruyama, K., Mizoi, J., Shinozaki, K., and Yamaguchi-Shinozaki, K. (2010). AREB1, AREB2, and ABF3 are master transcription factors that cooperatively regulate ABRE-dependent ABA signaling involved in drought stress tolerance and require ABA for full activation. Plant J. **61:** 672–685.

Zentner, G.E., and Henikoff, S. (2013). Regulation of nucleosome dynamics by histone modifications. Nat. Struct. Mol. Biol. **20:** 259–266.

Zhou, J., Wang, X., He, K., Charron, J.B., Elling, A.A., and Deng, X.W. (2010). Genome-wide profiling of histone H3 lysine 9 acetylation and dimethylation in *Arabidopsis* reveals correlation between multiple histone marks and gene expression. Plant Mol. Biol. **72:** 585–595.

Zhou, S., Jiang, W., Long, F., Cheng, S., Yang, W., Zhao, Y., and Zhou, D.X. (2017). Rice homeodomain protein WOX11 recruits a histone acetyltransferase complex to establish programs of cell proliferation of crown root meristem. Plant Cell **29:** 1088–1104.